

1 **A new digital Lithological Map of Italy at 1:100.000 scale for geo-** 2 **mechanical modelling**

Francesco Bucci¹, Michele Santangelo¹, Lorenzo Fongo², Massimiliano Alvioli¹, Mauro Cardinali¹, Laura Melelli², Ivan Marchesini¹,

¹ Consiglio Nazionale delle Ricerche, Istituto di Ricerca per la Protezione Idrogeologica, via Madonna Alta 126, I-06128 Perugia, Italy

² Università degli Studi di Perugia, Dipartimento di Fisica e Geologia, Piazza dell'Università 1, I-06123 Perugia, Italy

Correspondence to: Michele Santangelo (michele.santangelo@irpi.cnr.it)

3
4 **Abstract.** Lithological maps contain information about the different lithotypes cropping out in an area. At variance with
5 geological maps, portraying geologic formations, lithological maps may differ as a function of their purpose. Here, we describe
6 the preparation of a lithological map of Italy **at the 1:100,000 scale**, obtained from classification of a comprehensive digital
7 database and aimed at describing geo-mechanical properties. We first obtained the full database, containing about 300,000
8 geo-referenced polygons, from the Italian geological survey. We grouped polygons according to a lithological classification
9 by expert analysis of the original 5,456 unique descriptions of polygons, following compositional and geo-mechanical criteria.
10 The procedure resulted in a lithological map with a legend including 19 classes, and it is linked to a database allowing ready
11 interpretation of the classes in geo-mechanical properties, and amenable to further improvement. The map is mainly intended
12 for statistical and physically based modelling of slope stability assessment, geo-morphological and geo-hydrological
13 modelling. Other possible applications include geo-environmental studies, evaluation of river chemical composition,
14 estimation of raw material resources.

15 **1 Introduction**

16 Lithology encodes information on the composition and physical properties of rocks and, therefore, it is a key variable in the
17 study of earth surface and subsurface processes. As such, lithological analysis is relevant to a large body of literature, including
18 landscape evolution (Coulthard, 2001), water flow paths (Gleeson et al., 2011), landslides (Alvioli et al., 2021; Sarro et al.,
19 2020; Reichenbach et al., 2018), chemical composition of rivers or atmospheric CO₂ consumption (Donnini et al 2020;
20 Hartmann et al., 2010; Gibbs, 1994), soil classification (de Sousa et al., 2020), soil erosion (Vanmaercke et al., 2021), seismic
21 amplification (Mori et al., 2020; Forte et al., 2019), groundwater level variability (de Graaf et al., 2017; Lorenzo-Lacruz et al.,
22 2017), floods (Vojtek & Vojteková, 2019), oil reservoirs (Han et al., 2018), geothermal potential (Roche et al., 2019), geo-
23 morphological classification (Alvioli et al., 2020) and many others. Lithological variability is often a measure of geological

24 and landscape complexity, and provides important information on geological evolution and heritage (Bucci et al., 2019; Ispra
 25 & Parco Nazionale del Cilento, Vallo di Diano e Alburni, 2013, Santangelo et al., 2013), geo-resources settings (Bucci et al.,
 26 2016a; Ge.Mi.Na., 1962; Corpo Reale delle Miniere 1926-1935) geo-environmental risks (Giustini et al., 2019; Bentivenga et
 27 al., 2004) and matter fluxes at the Earth's surface (Brogi & Liotta, 2011; Boni et al., 1984).
 28 Lithological heterogeneity should be therefore sufficiently represented in maps at the local, regional and supra-regional scale.
 29 Lithological information is commonly derived from geological maps. In recent years, much effort has been made to make the
 30 geological data available around the world accessible at the best possible scales (Table 1, ID 1, 2). However, this still remains
 31 an open challenge because the quality, scale, updating and availability of geodata varies enormously across the globe.

32

ID	Services/products/data	Type	URL	Institutions	Context
1	<i>Visualization of the Geological map of the world at the best possible scales</i>	WebMap	http://portal.onegeology.org/OnegeologyGlobal/	Onegeology	Global
2	<i>General geologic map of the world at approximately 1:35,000,000 scale</i>	WebMap	https://mrdata.usgs.gov/geology/world/map-us.html#home	Geological Survey of Canada	Global
3	<i>Geologic Map Databases for the United States</i>	WMS, WFS, Download vector data	https://mrdata.usgs.gov/geology/state/	USGS	(Sub-) Continental USA
4	<i>Pan-European and national geological datasets and services from the Geological Survey Organizations of Europe</i>	WMS, WFS, Download vector data	http://www.europe-geology.eu/onshore-geology/geological-map/	EuroGeoSurvey	(Sub-) Continental Europe
5	<i>Geoportal of the Italian Geological Survey (ISPRA)</i>	WMS, WFS, Download vector data	http://sgi2.isprambiente.it/viewers/gi2/	ISPRA	National Italy
6	<i>Visualization of the available (in raster format) geological sheets of Italy at 1:100.000 scale</i>	Web application	http://sgi.isprambiente.it/geologia100k/	ISPRA	National Italy
7	<i>Visualization of the available (in raster format) geological sheets of Italy at 1:50.000 scale</i>	Web application	https://www.isprambiente.gov.it/Media/carg/index.html	ISPRA	National Italy
8	<i>Guidelines for the realization of the Geological and Geotechnical Map at the scale 1:50.000</i>	Web Page	https://www.isprambiente.gov.it/en/projects/soil-and-territory/carg-project-geologic-and-geothematic-cartography	ISPRA	National Italy
9	<i>REST service provided by ISPRA for the publication of spatial data</i>	REST	http://sgi2.isprambiente.it/arcgis/rest/services/servizi/carta_geologica_100k/MapServer/	ISPRA	National Italy

33 **Table 1:** Uniform Resource Locators (URL) of the institutional services, guidelines, products or datasets consulted for compiling our map.

34

35 The situation is more homogeneous at the continental or sub-continental level. For example, in 2017 the U.S. Geological
 36 Survey published a compilation of the individual releases of the Preliminary Integrated Geologic Map Databases (SGMC) for
 37 the United States (Table 1, ID 3), which represents a seamless, spatial database of 48 State geologic maps that range from
 38 1:50,000 to 1:1,000,000 scale (Horton, 2017). The SGMC is not a truly integrated geologic map database because geologic
 39 units have not been reconciled across State boundaries. However, the geologic data contained in maps for individual States
 40 have been standardized to allow spatial analyses of lithology, age, and stratigraphy.

41 In Europe, in 2016 the EuroGeoSurvey launched the European Geological Data Infrastructure (EGDI, Table 1, ID 4). EGDI
42 provides access to Pan-European and national geological datasets and services from the Geological Survey Organizations of
43 Europe. Geological Layers available include the Geological map of Europe, 1:5,000,000 scale, and the surface lithology of
44 Europe, 1:1,000,000 scale. More detailed geologic or geological derived maps are available at national scale **only** (Table 1, ID
45 5, 6).

46 In Italy, the existing geological maps with national coverage (Console et al., 2017) are at 1:1,250,000 (Bonomo et al., 2005)
47 1:1,000,000 (Pantaloni, 2011; Cipolloni et al., 2009; Compagnoni, 2004), 1:500,000 (Compagnoni et al., 1976-1983), and
48 1:100,000 scale (Servizio Geologico d'Italia, 2004) and are managed by ISPRA (Istituto Superiore per la Protezione e la
49 Ricerca Ambientale - De Logu et al., 2012). The 1: 50,000 national geological map, coordinated and published by ISPRA, has
50 an incomplete coverage of the Italian territory (Table 1, ID 7, 8).

51 Some of the **above mentioned** maps are accessible, for display purposes only, via standard view services (WMS -Web Map
52 Service, Table 1, ID 5).

53 Amanti et al., (2007) and (2008), described the first known attempt by ISPRA to draft a lithological map of Italy at the
54 1:100,000 scale. The published map covers the 65% of the national territory and does not include Sardinia, Sicily and the
55 sheets 156 to 176, 183 to 187 and 196 to 199. This lithological map is not accessible in raster or vector format.

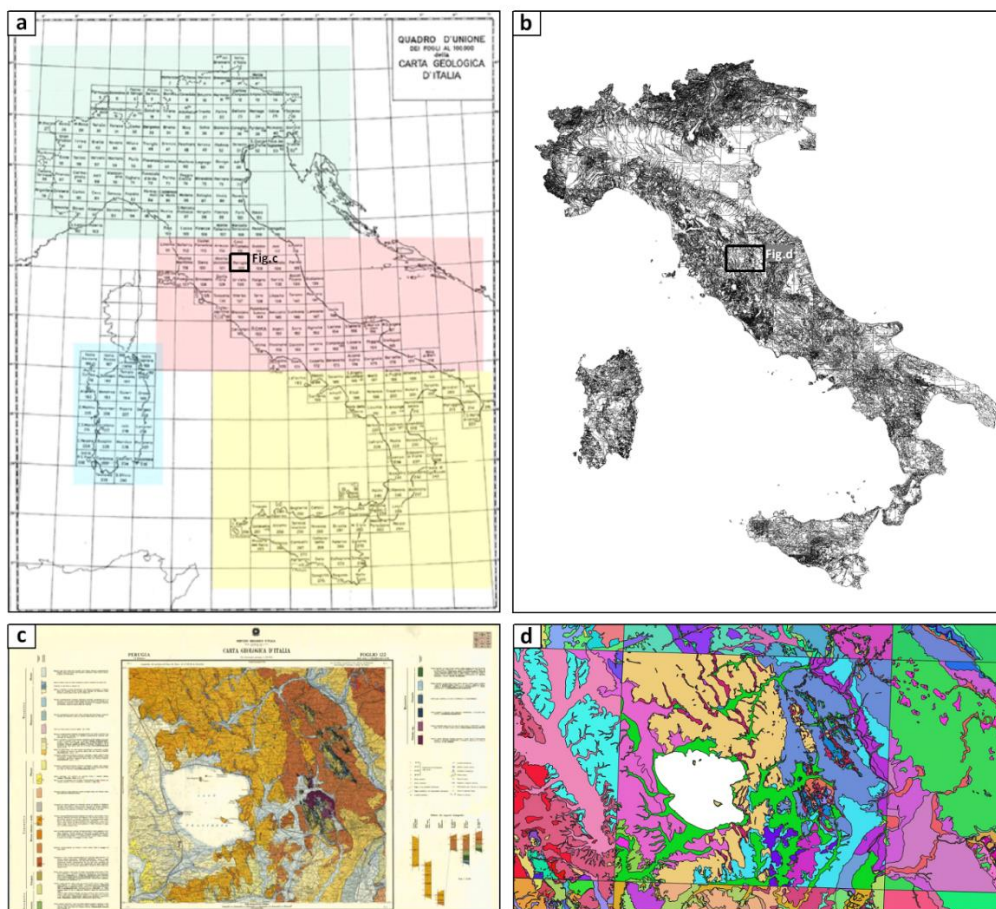
56 In 2018, ISPRA completed the work published in the 2007 and 2008 publications, and a lithological cartography of the entire
57 Italian territory at 1:100,000 scale, was made accessible for visualization, through the geo-portal (Table 1, ID 5). The map
58 was obtained gathering information from the 277 sheets of the Carta Geologica d'Italia, adopting a unique legend model to
59 produce a homogeneous lithological map of the **entire** country.

60 However, specific applications in different geosciences fields require distinct criteria and methods to elaborate different
61 lithological classifications. For example, starting from the geological maps produced by ISPRA at the 1:100,000 scale, a geo-
62 lithological map of Italy was recently classified according to the expected seismic behaviour of the material (Forte et al. 2019),
63 although the map is only represented as a figure along the paper, and not available for download or visualization.

64 Here, we describe a new lithological map of Italy (LMI), entirely available for download, aimed at differentiating lithotypes
65 based on their expected geo-mechanical properties in relation to slope stability and with the specific purpose of being used in
66 statistically based (Reichenbach et al., 2018; Schlogel et al., 2018; Alvioli et al., 2016; Rossi et al., 2016) and physically based
67 (Alvioli et al., 2021, 2016; Mergili et al., 2014; Raia et al., 2013) slope stability models. Early versions of the map described
68 in this work were used for geo-morphological analysis and terrain classification (Alvioli et al., 2020) and for rockfall
69 susceptibility assessment (Alvioli et al., 2021). The map and the associated database were designed in a versatile way. They
70 can be easily enhanced/reclassified using different or additional criteria, e.g., considering age, tectonic or geotechnical
71 information, and thus can be relevant to a wide range of studies.

72 2 Data

73 LMI was prepared starting from the data of the 277 sheets of the geological map of Italy at 1:100,000 scale (Table 1, ID 6),
74 provided by the Italian Institute for Environmental Protection and Research (ISPRA – Italian Geological Survey; *Servizio*
75 *Geologico d'Italia*, 2004) available as a digital database through the ISPRA website. The website exhibits a representational
76 state transfer (REST) service for the publication of spatial data (Table 1, ID 9), and distributes the geological map of Italy at a
77 scale of 1:100,000, in vector format (Figure 1). The map contains 294,266 topologically correct polygons, and 5,477 unique
78 descriptions of the geological formations. The scanned versions of the original geological sheets are also available for
79 consultation (Table 1, ID 6).



80

81 **Figure 1:** (a) The 277 sheets of the geological map of Italy at 1: 100,000 scale as visualized at the ISPRA website (Table 1, ID 6). The
82 location of figure (c) is indicated; (b) All the unclassified 292,705 vector polygons available in the source dataset. The location of figure (d)
83 is indicated; (c) Published version of the sheet n. 122 “Perugia” as visualized in raster form at the ISPRA website (Table 1, ID 6); (d)
84 Randomly coloured polygons within the area encompassing the sheet n. 122. Polygons having the same geological description in the original
85 attribute table (field: NAME) provided by ISPRA (Table 1, ID 9) assume the same colour. The area also encompasses the straight boundaries
86 with its surrounding four geological sheets, clearly visible as sharp colour changes along NS and WE oriented straight lines.

87

88

89 The attribute table associated with the polygons originally contained a unique numeric identifier and the description of the
 90 geological unit as specified in the original geological maps (field: *NAME*). Comparison between the original legend
 91 descriptions and the text reported in the description field revealed that several simplifications were made. Such differences
 92 represented a major source of inhomogeneity within the database, which limited the efficacy of using automated database
 93 queries to apply the new lithological classification scheme. Table 2 reports examples of such simplifications of the original
 94 legend.

95

Simplifications and Problems in the Name_Ulf column	NAME Descriptions	Geological Sheet numbers	Approach to the issues	Original Descriptions
<i>Lack of information concerning the name of the formation, the lithology and the internal architecture</i>	undifferentiated	92-93	SQ+ancillary	Sericitic, quartz-sericitic, chloritic schists, of Permian age, prevalent, not separable cartographically from schistose limestones because of the minute mixture determined tectonically
<i>Lack of information concerning the name of the formation and the lithology</i>	lenticular alternations	130	SQ+ancillary	Lenticular alternations, of variable extension and power, consisting of: clay and varicolored marl, calcarenite, calcareous breccia, sandstone, limestone and marly limestone.
<i>Lack of information concerning the lithology</i>	Corleto Perticara formation	200	SQ+ancillary	Violet, brown and yellowish clayeyes, gray and white clayey marls, subordinately red, calcareous marls and marly limestones of gray or greenish color, gray calcarenite or gray quartzarenites with siliceous cement.
<i>Only partial lithological information</i>	Corleto Perticara formation - marne	199	SQ+ancillary	Clayey marl gray and subordinately red; calcareous marl and marly limestone of gray or greenish color, calcarenite and sandstone.
<i>Identification of a rock unit with local/informal denomination</i>	“metallifero bergamasco”, “biancone”	7-18 35, 36, 49, 22,38	SQ+ancillary	Well stratified black limestones, often with parallel lamination and pisolithic at the base; dolomite intercalations in the lower part. White compact limestones; greyish or gray limestone; black marly, bituminous limestone; greenish marl; ceroid limestones with chert.
<i>Formations made up of several members</i>	sandstones, quartzites, phyllites, schistose sandstones, argilloscist	226	SQ+ancillary	Sandstones, quartzites, phyllites, schist sandstones, more or less phylladic clayey, alternating, sometimes even minute.
<i>Typos</i>	“scisti di ?dolo”	7-18	Q	“Scisti di Edolo”
<i>Singular/plural</i>	moraine/moraines	30, 31, 32, 17, 20, 12, 132, 140, 145, 151, 152, 160, 209, 210 /151	Q	Moraine/Moraines
<i>Uppercase/lowercase</i>	Moraine/moraine	62/25, 24, 22, 4 ^b , 22, 6, 8, 18, 19, 33, 34, 5, 15, 16, 27, 28, 29, 41, 55, 66	Q	Moraine

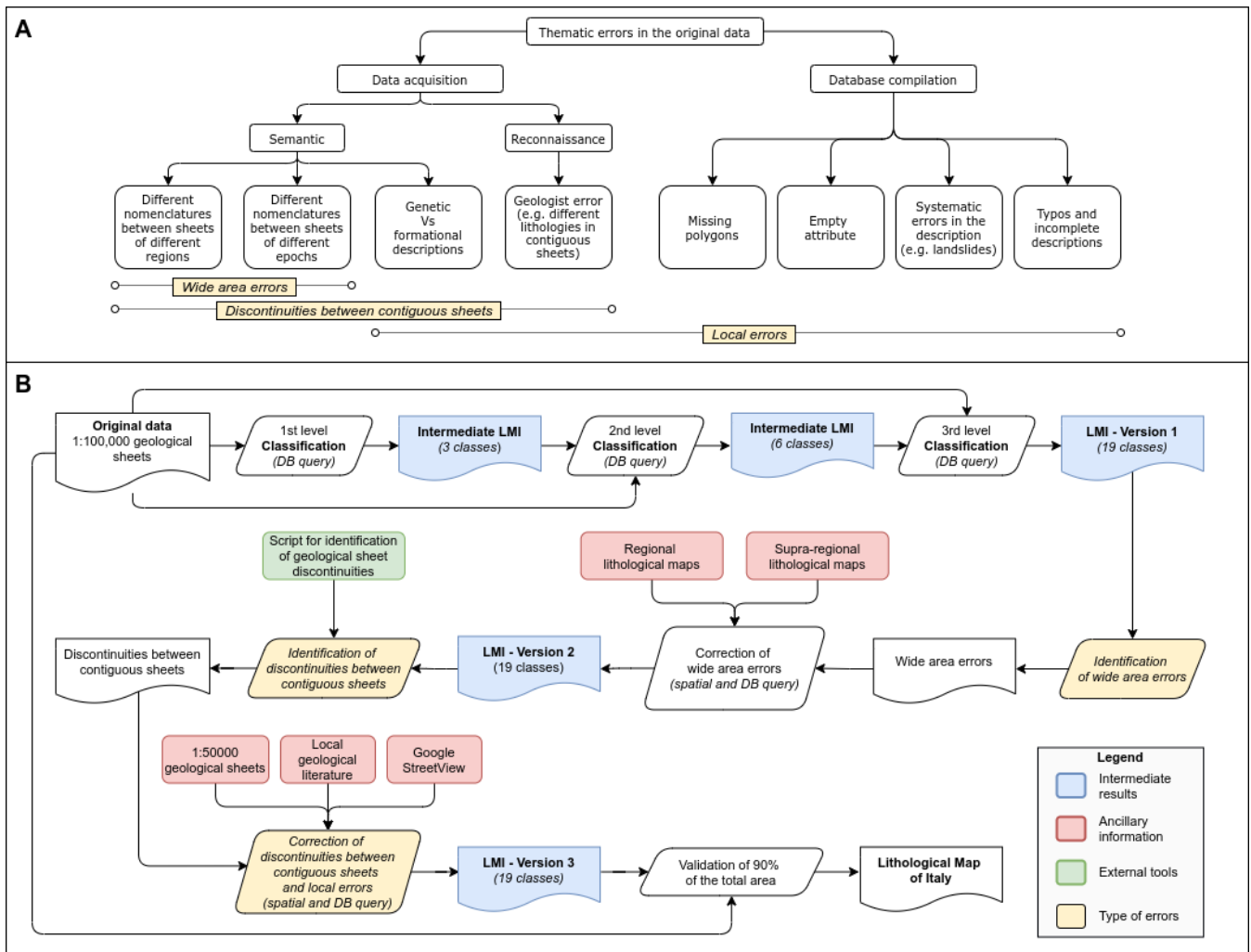
<i>Mangled names in some sheets</i>	“majolica” in place of “maiolica”	139	Q	“Majolica”
<i>Spelling errors</i>	“ammessi subvulcanici”	11	Q	“Ammassi subvulcanici”
<i>Use of accents</i>	“unità di sillano”	108	Q	“Unità di Sillano”
<i>Use of apostrophes</i>	“marne e calcari dell'antola”	84, 85	Q	“Marne e calcari dell'Antola”
<i>Use of percentage</i>	soils containing more than 10% of organic substances	76	Q	Soils containing more than 10% of organic substances
<i>Use of special character letters</i>	würmian moraines	54, 42, 67, 4, 1-4 ^a , 14, 14 ^a , 91	Q	Würmian Moraines

Table 2: Examples of simplifications and problems related to the unique rocks descriptions contained in the source dataset, and comparison with the original description in the legend of the original geological sheets. Depending on their nature, issues were approached using database queries (Q), spatial queries (SQ), and ancillary material (regional/local geological maps and literatures).

96
97
98
99

100 In most cases, the text corresponds only to the first word or lemma of the original description. In the case of formations made
101 up of several members, the *NAME* field contains a lemma indicating the main lithological members, but this approach is not
102 consistent for all records. In some cases, the polygons correspond to empty records in the attribute table (most of them refer to
103 lakes or inland waters); in others, the polygons are absent and were added in this work to fill in empty areas, according to the
104 information checked in the original geological sheets. Overall, the analysis of the database revealed several types of errors
105 affecting the source data set, which are summarized in Figure 2a. We refer to errors in the database as *thematic errors*, since
106 the attribute assigned to a polygon is incorrect or not corresponding to the ground truth (assumed here to be the original
107 geological sheets). Thematic errors in the database can be grouped according to two main categories: *inconsistency between*
108 *surveyors*, and *errors of the operators* who compiled the database. We refer to the first as to “Data acquisition errors” and to
109 the second as to “Database compilation errors”.

110 *Data acquisition errors* are related to individual mapping errors (*Reconnaissance errors*, in Figure 2a) or to disused, or
111 dialectal/jargon geological descriptions (*Semantic errors*, in Figure 2a). Figures 3a and 3c show typical errors related to
112 subjectivity issues visible at the boundary between geological sheets drafted by different working groups and published many
113 years apart from each other (Console et al. 2017). Figure 3c also contains references to local or dialectal terms that may escape
114 general lithological classification criteria. Subjectivity errors related to disused, inadequate or dialectal geological description
115 and terms were systematically resolved (Figure 3d) by using database queries. Despite our effort, little or nothing could be
116 done for most of the errors due to contrasting classification of rock assemblages by individual geologists or the working groups
117 who compiled the original geological sheets. Such problems still remain in our lithological map (Figures 3b,d). A new national
118 geological survey currently in progress (Carg project, Table 1, ID 7, 8) will likely resolve critical information of geological
119 interpretation, which is beyond the scope of this work.



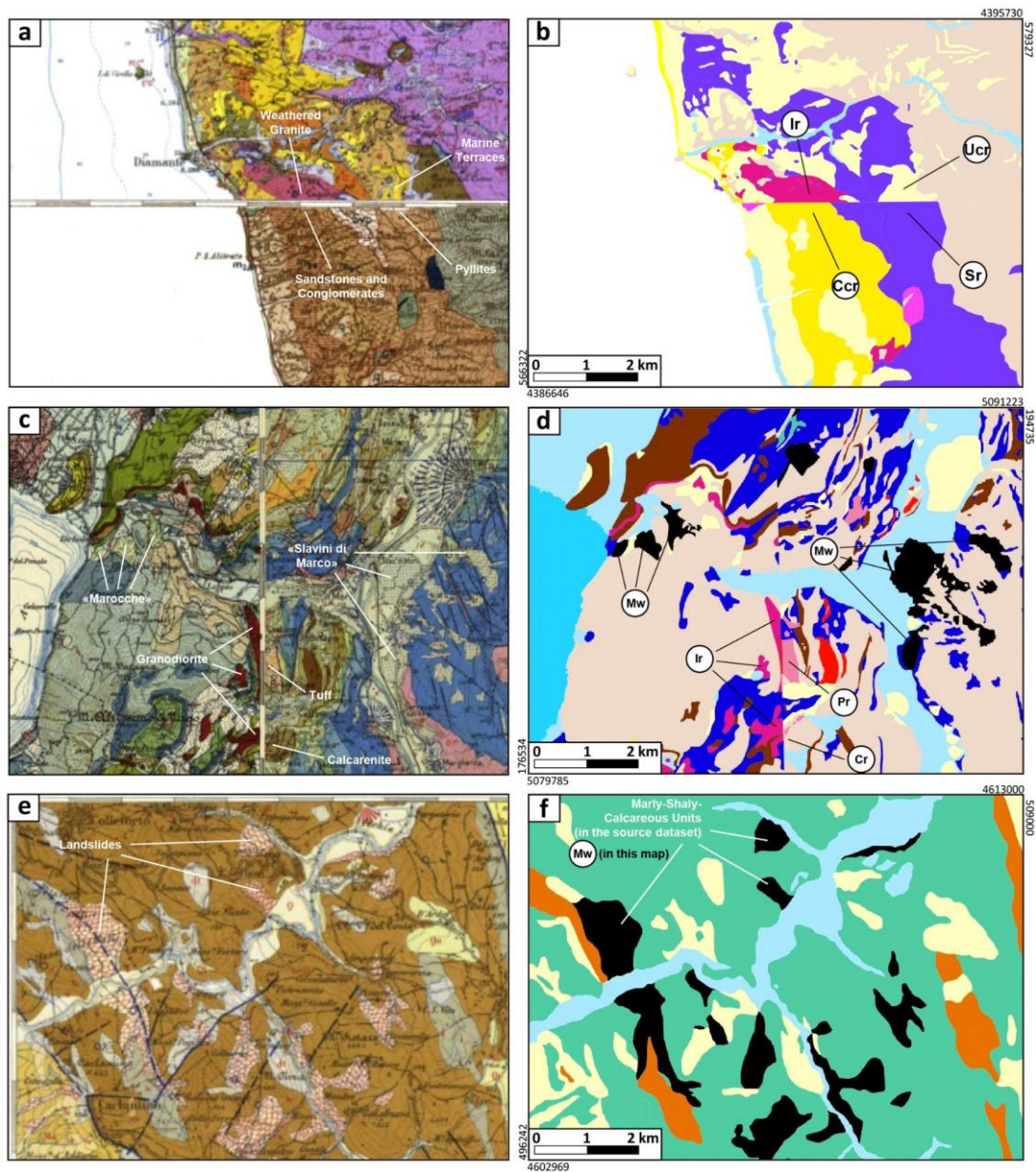
120

121 **Figure 2:** (a) Scheme of the main thematic errors identified in the source dataset. Errors can be related to (i) uncorrected or incomplete
 122 database compilation or (ii) to data acquisition as a consequence of individual errors or inhomogeneity in the use of geological nomenclature,
 123 description and interpretation; (b) Flowchart of the classification process of the Lithological Map of Italy

124

125 *Database compilation errors* can be systematic (Figure 3f) and occasional. Figure 3f refers to a systematic thematic error
 126 dealing with the compilation of the *NAME* column of some landslide polygons with the description of a lithostratigraphic unit
 127 clearly unrelated to landslides. As exemplified in Figure 3f, the compilation errors were identified and corrected during the
 128 reclassification of the source dataset.

129



130

131 **Figure 3:** Main problems of the source dataset highlighted through the comparison of representative areas, as appear respectively in the
 132 published raster version of the geological sheets (**a, c, e**) and in the our reclassified vector map (LMI) (**b, d, f**) - Vector Map Legend - Ir
 133 (Intrusive rocks), Ucr (Unconsolidated clastic rocks), Ccr (Consolidated clastic rocks), Sr (Schistose rocks), Pr (Pyroclastic rocks), Cr
 134 (Carbonatic rocks), Mw (Mass wasting); Example of errors related to locally wrong rocks classification and inhomogeneity problems at the
 135 boundary between geological sheets of different years are shown in (a) (year 1969 - N sheet n. 220 vs year 1890 - S sheet n. 228) and in (c)
 136 (year 1948 - W sheet n. 35 vs year 1966 - E sheet n. 36); Examples of local/dialectal terms in the geological description are shown in (c)
 137 (“Marocche” and “Slavini di Marco” for Mass wasting); Examples of errors related to incorrect database compilation are shown comparing
 138 (e) and (f). Figures **a, c, e**, include sheets number **220, 228, 35, 36, 163** as visualized in raster form at the ISPRA website (Table 1, ID 6).

139 3 Methods

140 The procedure used to compile out the new Lithological map of Italy (LMI) is described in Figure 2b. Starting from the original
141 data (top left in Figure 2b) we derived the LMI (bottom right in Figure 2b) through the following steps: (a) definition of a
142 procedure including alphanumeric queries, geospatial analysis and expert judgements; (b) preparation of at least two
143 intermediate products and three versions of the LMI.

144 The “*Intermediate LIM - 3 classes*” product (Figure 2b) follows a genetic criterion and describes (i) magmatic, (ii)
145 metamorphic and (iii) sedimentary rocks.

146 The “*Intermediate LIM - 6 classes*” product (Figure 2b), distinguishes (i) older (typically Pre-Neogene in age) and structured
147 substratum-derived sedimentary rocks and (ii) magmatic intrusion, from (iii) younger (Neogene and Quaternary in age) less-
148 to-not deformed sedimentary and magmatic cover rocks. Sedimentary cover was further separated in (iv) undifferentiated and
149 (v) alluvial/marine rocks, while the (vi) metamorphic rocks class remains unchanged.

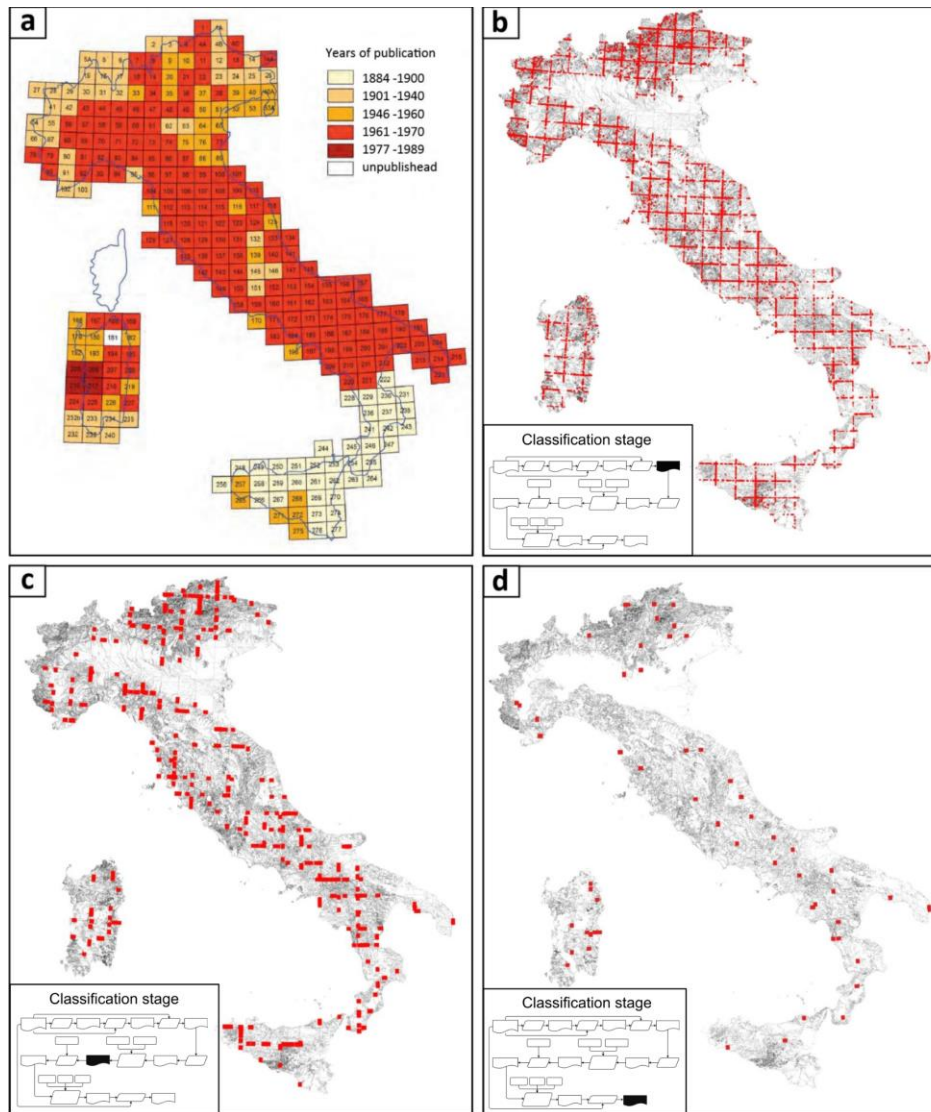
150 “*LMI - Version 1*” (Figure 2b) is based on a predominantly lithological criterion, and contains the 19 classes defined in our
151 legend.

152 To translate different rock type information into lithological classes, the dominant rock types were emphasized assuming that
153 rocks mentioned foremost are more abundant than those mentioned later in the descriptions. This classification strategy is
154 consistent with many mapping guidelines (UNESCO-IUGS, 2016; Hartmann et al., 2012; Asch, 2005), and is based on the
155 classification system by Dürr et al. (2005), with modifications. Determining the dominant rock types within a unit was not
156 always straightforward, though. Cases of uncertainty about the dominant rock type were found and were resolved by
157 considering specific lithological classes defined by the combination of the most representative rock types. For example, the
158 rock unit named “Clays and Limestones”, composed in equal parts of both lithotypes, was assigned to the class “mixed
159 sedimentary rocks”, which also contains other sediments where carbonates are mentioned but not dominant.

160 Each classification step (“1st, 2nd, 3rd level” in Figure 2b) used the result of the former step (where applicable) and the original
161 data to build complex alphanumeric database queries. No spatial queries were involved. Furthermore, the first two (coarser)
162 levels of classification (intermediate products) helped underlining systematic semantic and compilation errors throughout the
163 database. For example, rock units containing the word “schist” were consistently classified as “metamorphic rocks” in the first
164 level classification, which led to classifying sedimentary rocks with a strong pelitic component as metamorphic rocks. This
165 happened since such sedimentary rocks were commonly improperly indicated as “schists” in geological descriptions dating
166 over 50 years. Similarly, the words “clays” and “claystones”, or “sands” and “sandstones”, were sometimes used as synonyms
167 in the original geological legend, with consequent uncertainty between the sedimentary cover or the sedimentary substratum.
168 Inconsistencies of the source data set mainly derive from the large variability of the level of detail of the original geologic
169 descriptions between different geological sheets. Compilation of the 277 geological sheets of the entire National territory

170 required 92 years, from 1884 to 1976 (Figure 4a), which inevitably led to differences in the geological descriptions (and
171 interpretation) between old and recent sheets.

172



173

174 **Figure 4:** (a) The 277 sheets of the geological map of Italy at 1: 100,000 scale classified according to the years of publication, as visualized
175 in Console et al., 2017, Figure 3; (b) The 12711, NS-EW oriented segments (red lines) having different lithotypes in the two sides and
176 sinuosity equal to 1. (c) The 405 Red lines longer than 1000 m left after semi-automatic classification. The unclassified 294,266 vector
177 polygons of the source dataset are shown as background in (b) and (c); (d) the 58 Red lines longer than 1000 m left after the expert analysis
178 of the semi-automatic output. The unclassified 100,705 vector polygons derived from the dissolve GIS operation performed after the
179 classification phase are shown as background. Insets in (a), (b), and (c) indicate the classification stage to which each map refers, according
180 to the scheme in figure 2b.

181

182 A similar issue was introduced between sheets or regions mapped by different authors and working groups (Figures 3a,c). As
183 a consequence, problems of inhomogeneity were found in the descriptions of litho-stratigraphic units, which in turn generated
184 problems of harmonization at the boundary between different geological sheets. To mitigate inhomogeneity problems, we
185 decided to adopt broad categories in the classification of the third level as a function of similar lithology, genetic processes
186 and expected geotechnical behaviour. With this aim, rock descriptions were generalized into 19 lithological classes. However,
187 harmonizing the original 5,477 univocal descriptions of the geological units in 19 simplified lithological classes was often
188 tricky and required expert judgement supported by the consultation of regional and supra-regional geo-lithological maps (Conti
189 et al., 2020; Piana et al., 2017; Lentini & Carbone, 2014; Carmignani et al., 2013; Vezzani et al., 2010; Celico et al., 2005;
190 Carmignani, 2001; Consiglio Nazionale delle Ricerche, 1990; Amodio Morelli et al., 1976). We used a very long and complex
191 set of database queries to classify and harmonize the data. For example, to correctly classify glacial drift avoiding possible
192 overlapping with alluvial deposits, we requested the NAME field to either contain strings with the words "wurm", "würm",
193 "glacial", "moraine", and at the same time without any of the words "alluvial", "fluvial" and "terrace". Due to their specificity,
194 queries were generally longer and more complex when used to classify widespread lithological classes containing a large
195 number of unique descriptions. The *LMI - Version 2* is the product of this harmonization phase where "wide area errors" were
196 corrected (Figure 2b), resulting in a lower number of discontinuities at the boundaries of regions or individual geological
197 sheets, compared to these contained in the *LMI _Version 1* (Figure 4 b,c).

198 To identify discontinuities between contiguous geological sheets (Figure 2b) we developed an automatic procedure based on
199 the analysis of the lithological classes located to the right and left of each lithological boundary. We selected all EW and NS
200 oriented straight boundaries longer than 1 km and resolved classification inconsistencies across such boundaries by expert
201 **advice**. Discontinuities between contiguous geological sheets are due to inconsistencies between surveyors. Since we assumed
202 that the ground truth is the original geological sheets, our approach consisted in assuming only one of the two contiguous
203 polygons was to be corrected. If available ancillary data allowed to confirm one of the two bounding polygons attribute,
204 classification of the second polygon was amended accordingly. Otherwise the discontinuity was solved by assigning the class
205 that minimised discontinuities and inconsistencies.

206 To reduce the number of discontinuities between contiguous sheets, we consulted geologic maps available at **the** 1:100,000
207 **scale** (Servizio Geologico d'Italia, 1970a,b,c,d,e, 1969, 1968a,b, 1965, 1964, 1955; Ministero dei Lavori Pubblici, Ufficio
208 Idrografico, Sezione Geologica, 1948; R. Ufficio Geologico, 1884a,b,c,d,e, 1900) and at **the** 1:50,000 **scale** (Servizio
209 Geologico d'Italia, 2016, 2015a,b,c, 2014, 2012a,b,c, 2011a,b,c,d, 2010a,b,c, 2009a,b, 2008, 2006, 2005a,b,c,d, 2002, 1973,
210 1972), where available. Where information on rock types was unavailable from the national maps, we obtained the descriptions
211 of the named stratigraphic units from regional and local geological maps and from the scientific literature (Novellino et al.,
212 2021; Bucci et al., 2020, 2016, 2014, 2012; Vignaroli et al., 2019; Mirabella et al., 2018; Ronchi et al., 2011; D'Ambrogi et
213 al., 2010; Brozzetti, 2007; Chiarini et al., 2008; Giannandrea et al., 2006; Schiattarella et al., 2005; De Rita et al., 2004; Girotti

214 & Mancini, 2003; Catanzariti et al., 2002; Bortolotti et al., 2001; Prosser, 2000; Giardino & Fioraso 1998; Tavarnelli, 1997;
215 Campobasso et al., 1994; Centamore et al., 1991; Patacca et al., 1991; Calamita et al., 2009; Centamore et al., 2009; Gueguen
216 et al., 2010; Tavarnelli et al., 2003a, b). The quality of the literature was variable, and may have introduced some uncertainty.
217 In some rare locations, the rock type information of digital geological map vector datasets was derived from paper maps, which
218 were georeferenced and visually assigned to the units of the digital maps. In specific and rare cases, it was necessary to use
219 geographic visualization software, such as Google Earth and Google Street View, to study and display images of outcrops for
220 a local visual analysis. After this finer phase of correction, a total of 58 segments longer than 1000 m remained unsolved since
221 they would require the geometry of the original polygons to be modified (Figure 4d). The problem greatly increases for the
222 classification inconsistencies along segments shorter than 1,000 meters, for which a systematic correction was out of the scope
223 of this work.

224 After the classification phase, boundaries were dissolved to merge adjacent polygons sharing the same lithology. With this
225 streamlining operation, the number of polygons has dropped from 294,266 to 180,503. The result of the correction of
226 discontinuities between contiguous sheets is the *LMI - Version 3* (Figure 2b).

227 Eventually, we performed a validation of the map *LMI - Version 3* (Figure 2b). First, the area percentages of all the unique
228 descriptions within each class were computed and sorted in descending order. Then, within each lithological class, all the
229 unique descriptions summing to a total area of 90% of that class were inspected for possible inconsistencies, by comparing
230 and verifying the assigned lithology with the original description in the field NAME. The total area validated corresponds to
231 271,651.56 km², which represents ~90% of the Italian territory and includes 1,702 different geological descriptions. For each
232 lithological class, polygons of a very small size, between 0.05% and 0.8% of the area of the lithological class itself, were
233 validated (Table 3). The remaining 10% of the total area of each lithological class, which consists of 4,632 records associated
234 with negligible percentage values of the area (on average 0,06% of the total area of each class), was not checked. It is worth
235 noting (Table 3) that the Carbonate rocks class (Cr) accounts for most of the descriptions (1,155), followed by Unconsolidated
236 clastic rocks (Ucr), Alluvial and marine deposits (Al) and Siliciclastic sedimentary rocks (Ssr) which include 856, 583 and 560
237 descriptions respectively. However, the areal extent of these four classes (the most represented on the territory) does not reflect
238 the number of descriptions, as the most extensive class is Al (75,424.36 km²), followed by Ucr (45,764.12 km²) and then Cr
239 and Ssr (45,329.81 km² and 34,099.68 km², respectively).

240 We checked all of the records classified as anthropogenic deposits (12 records), landslides (26 records), lakes and glaciers (10
241 records) (Table 3). Some errors inherited from compilation errors of the source dataset, also emerge from the validation as
242 classification inconsistencies. To give an example of this kind of errors we report a case from the landslide class, in which the
243 most representative (21% of the area, with respect to the total landslide class) unique descriptions are defined as “clayey and
244 calcareous turbidites of Paleogene age”. These same polygons were, instead, correctly represented as landslides in the original
245 geological sheet in raster format (Figure 3e). Wherever possible, polygons classified as landslides were manually corrected by

246 looking at the original raster map. Similar errors concerning other geological descriptions were treated using the same
 247 approach. After validation, the final *Lithological Map of Italy* (LMI) was produced (Figure 2b).

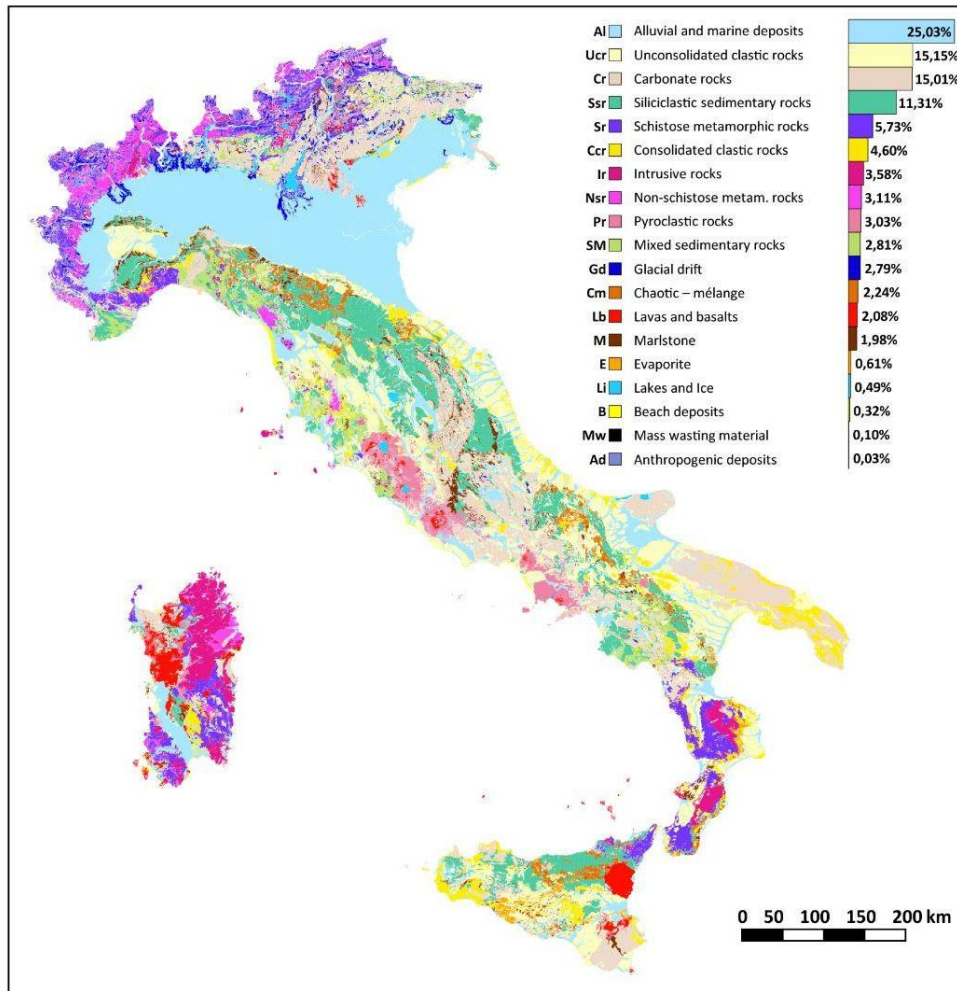
Lithologic class	N. object (#)	A. min (m ²)	A. max (km ²)	A. med (km ²)	A. tot (km ²)	N. description (#)	N. description checked (#)	A. description checked (%)	A. min checked (%)
<i>Sr</i>	13,040	50	1909.83	1.32	17,296.50	436	93	90	0.18
<i>Nsr</i>	14,595	263	994.09	0.64	9351.25	382	100	90	0.17
<i>Ir</i>	11074	56	4238.05	0.97	10,778.27	363	55	90	0.22
<i>Pr</i>	5508	239	2447.07	1.66	9121.65	360	112	90	0.18
<i>Lb</i>	7735	259	1227.15	0.81	6256.87	336	85	90	0.21
<i>Cr</i>	21,070	16	4836.92	2.15	45,329.81	1155	304	90	0.05
<i>M</i>	8541	23	243.65	0.70	5964.80	235	78	90	0.21
<i>SM</i>	5382	216	921.16	1.57	8455.40	181	66	90	0.35
<i>Cm</i>	4167	58	911.52	1.62	6752.96	114	25	90	0.67
<i>Ssr</i>	11,930	24	3924.31	2.86	34,099.68	560	145	90	0.12
<i>E</i>	2634	989	238.72	0.70	1839.48	87	22	90	0.72
<i>Ucr</i>	37,641	32	1260.33	1.22	45,764.12	856	229	90	0.08
<i>Ccr</i>	8391	39	1392.17	1.66	13,915.05	397	112	90	0.16
<i>Gd</i>	11337	2145	318.28	0.74	8406.20	107	16	90	0.63
<i>Mw</i>	1231	33	9.18	0.26	315.72	26	26	100	0.02
<i>Ad</i>	125	1573	25.31	0.71	88.72	12	12	100	0.03
<i>Li</i>	329	1252	367.79	4.52	1485.44	10	10	100	0.01
<i>B</i>	968	136	105.96	1.01	978.80	79	35	90	0.60
<i>Al</i>	14,804	66	46,634.58	5.09	75,424.36	583	177	90	0.10

248
 249 **Table 3:** Descriptive statistics of the 19 lithological classes. In the left half of the table, the number of polygons, and their minimum,
 250 maximum, average and total area for each lithological class are shown. The right half of the table shows the number of total unique
 251 descriptions and those checked during the technical validation in relation to the percentage of the area covered by the validation (% of the
 252 total area) and the detail of the validation (minimum area checked)

253 **4 Results**

254 The main results of this work are: (i) the translation of the rock type information extracted from the stratigraphic units of the
255 geological maps of Italy at the 1:100,000 scale into lithological classes and (ii) the development of a data architecture open to
256 further improvement, aimed in particular at linking the lithological classes to their expected geotechnical behaviour.

257 The new *Lithological map of Italy* (LMI, this work) represents the first freely downloadable national distribution of the
258 different lithological classes at a high resolution. The map scale is 1:100,000. The assembled map consists of a total of 180,503
259 polygons distributed in 19 lithological classes (Figure 5).



260

261 **Figure 5:** Map of Italy showing the 19 lithological classes identified both with the short ID and the extended name.
262 Percentage distribution of each lithological class over the Italian territory is indicated and visualized in a bar chart.
263

264

265 The Italian surface is covered by 82,47% sediments (a third of which are alluvial deposits), 8,84% metamorphics, 3,58%
 266 plutonics, and 5,11% volcanics (Table 4). A specific class was assigned to areas of ice and inland water bodies, which cover
 267 0,49% of the map area.

268

Physiographic regions of Italy		Metamorphic		Magmatic			Sedimentary													← I level	
Acronym	Name	Substratum		Intrusion	Cover		Substratum					Undifferentiated Cover					Alluvial/ Marine			← II level	
		Sr	Nsr		Ir	Pr	Lb	Cr	M	SM	Cm	Ssr	E	Ucr	Cer	Gd	Mw	Ad	Li	B	Al
EAL	Eastern Alps	1.7	0.2	0.9	4.0	2.7	46.5	2.2	5.7	-	4.5	0.1	10.3	1.4	9.7	0.3	-	-	0.7	9.3	100
CAL	Central Alps	15.8	13.8	4.5	1.7	0.6	21.1	1.0	3.2	-	2.4	0.0	10.3	0.5	15.8	0.3	-	-	2.7	6.2	100
WAL	Western Alps	26.7	25.2	4.9	0.1	0.1	6.4	0.5	3.1	0.0	4.8	0.0	8.3	2.1	11.0	0.0	0.0	-	0.7	6.0	100
PP	Po Plain	0.0	0.1	0.1	0.2	0.1	0.2	0.1	-	0.0	0.4	0.0	1.7	0.4	3.6	-	0.2	0.0	0.5	92.5	100
NAP	Northern Apennine	1.0	1.5	0.2	-	0.0	6.7	5.6	9.6	10.2	39.0	0.7	11.3	3.3	0.3	0.2	0.0	-	-	10.3	100
NIAP	North-Internal Apennine	0.7	1.3	0.6	1.7	0.3	6.1	1.3	8.9	1.1	18.6	0.4	28.2	4.8	-	0.1	1.5	0.1	0.6	23.7	100
CEAP	Centre-Eastern Apennine	-	-	-	-	-	1.0	0.6	-	0.1	12.0	0.3	51.1	11.2	-	0.0	0.5	-	-	23.2	100
CAP	Central Apennine	-	-	-	3.1	0.1	47.6	9.4	0.0	0.0	14.7	0.0	11.4	2.2	0.4	0.0	0.0	0.0	0.1	10.9	100
CMP	Central Magmatic Province	0.0	-	-	58.4	9.3	3.4	0.1	0.4	-	0.2	0.0	13.0	0.8	-	0.0	0.0	0.0	3.0	11.3	100
SMP	Southern Magmatic Province	-	-	-	50.1	3.8	10.3	0.0	-	0.1	3.9	-	21.9	0.0	-	-	1.5	1.6	0.1	6.6	100
SAP	Southern Apennine	1.8	0.1	0.0	1.9	0.1	20.0	1.5	5.8	7.4	24.8	0.1	21.9	5.9	0.0	0.6	0.1	-	0.0	8.0	100
SEAP	South-Eastern Apennine	-	-	-	-	-	1.3	0.0	0.0	0.3	0.3	0.0	51.6	7.8	-	0.0	1.1	-	0.6	36.9	100
GF	Gargano Foreland	-	-	-	-	-	79.3	-	-	-	-	-	4.8	0.3	-	-	0.4	-	3.8	11.4	100
MF	Murge Foreland	-	-	-	-	-	59.7	-	-	-	-	-	12.1	24.4	-	-	0.2	-	-	3.6	100
WS	Western Sicily	0.1	-	-	0.0	0.0	10.0	2.5	0.4	7.0	26.6	6.5	24.1	13.6	-	0.0	0.1	-	0.0	9.0	100
ES	Eastern Sicily	-	-	-	2.8	21.8	27.1	2.4	-	0.5	1.7	0.9	25.0	3.5	-	-	0.3	-	-	14.1	100
CPA	Calabro-Peloritano Arc	29.0	0.2	14.4	0.3	0.3	2.4	2.7	0.0	2.3	4.8	2.2	22.2	9.0	-	0.0	-	-	-	10.3	100
SB	Sardinian Block	15.7	5.6	26.6	4.3	13.5	7.0	0.9	-	0.0	3.2	-	3.2	2.8	-	-	0.6	0.0	0.1	16.5	100
Total Italian territory III level →		5,73	3,11	3,58	3,03	2,08	15,01	1,98	2,81	2,24	11,31	0,61	15,15	4,60	2,79	0,10	0,03	0,49	0,32	25,03	100
Total Italian territory II level →		8,84		3,58		5,11		33,35					23,28					25,84			100
Total Italian territory I level →		8,84		8,69		82,47													100		

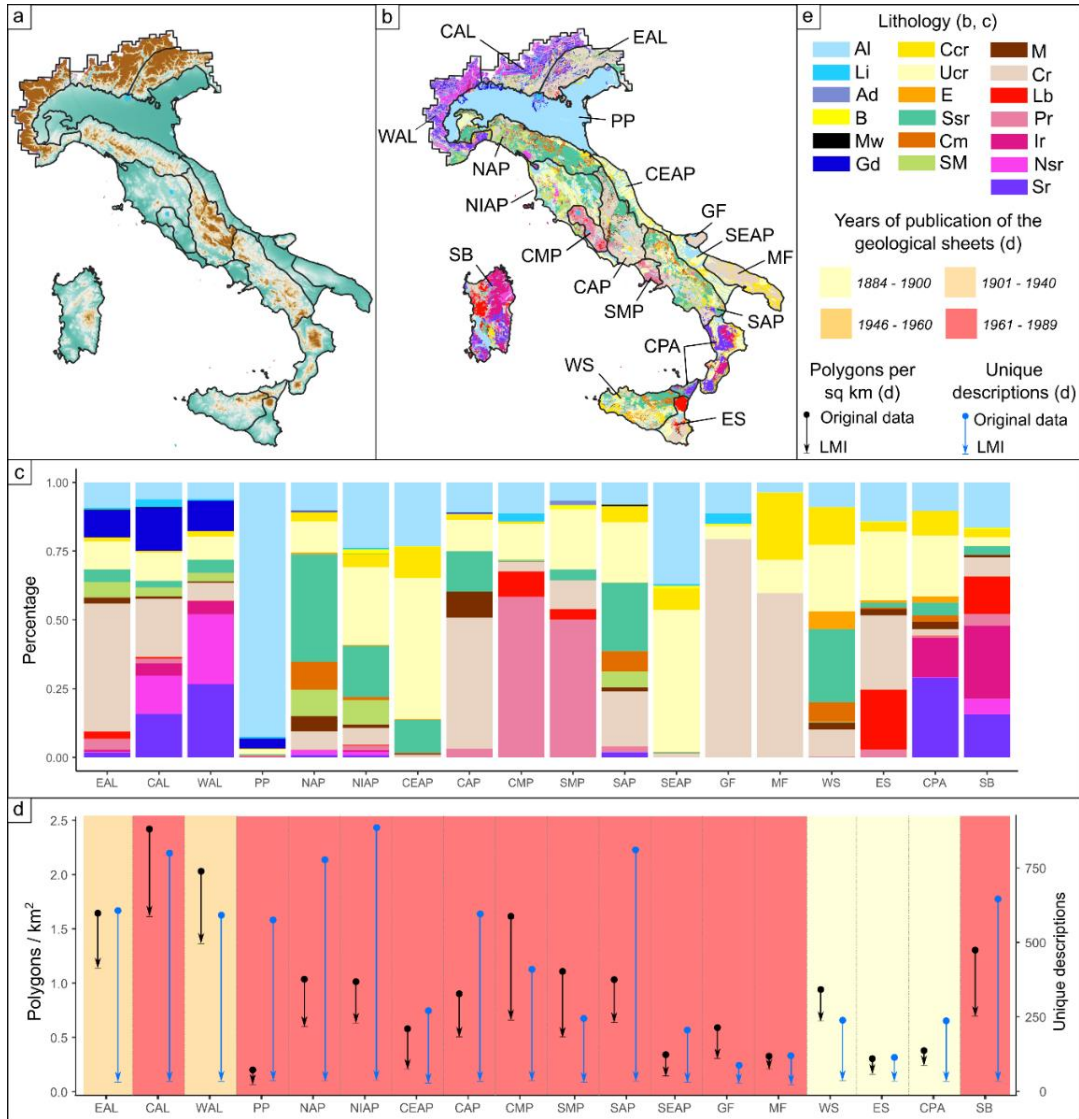
269 **Table 4:** Percentage distribution of the lithological classes (columns), organized in three hierarchically different levels of classifications,
 270 within the 18 physiographic regions of Italy (rows).

271 Below, the lithological classification describes the general rock types in each unit, in alphabetic order.

- 272 • **Alluvial deposits (Al):** alluvial, lacustrine, swamp and marine deposits. Eluvial and colluvial deposits.
- 273 • **Anthropogenic deposits (Ad):** include Roman and modern landfills, drainage channel excavations and
 274 archaeological remains.
- 275 • **Beaches and coastal deposits (B):** include beaches and coastal deposits.
- 276 • **Carbonate rocks (Cr):** carbonate-dominant sedimentary rocks. Examples of Cr units are limestone, dolomite and
 277 marl (but only where associated and in a clear minority with respect to limestone, otherwise they are included in class M). As
 278 usually the rock descriptions of the mapped units do not give relative abundances of the rock types which they encompass,
 279 units were classed as Cr if the first named rock type was a carbonate rock, if the majority of rock types were carbonates or if
 280 the named order otherwise led to the impression of a domination by carbonates.
- 281 • **Chaotic – mélange (Cm):** include chaotic terrains with a predominantly clay matrix and olistostromes composed by
 282 mixed sedimentary rocks (SM class). Fragments of ophiolite structures were locally included in the Cm class.

- 283 • **Consolidated clastic rocks (Ccr):** clay, sand, debris, conglomerates with a varied origin, usually of Neogene and
284 Quaternary age, which have undergone consolidation or secondary cementation phenomena.
- 285 • **Evaporite (E):** contains substantial amounts of evaporitic rocks. The typically **and most frequently** encountered
286 evaporite rock **is** gypsum, but also anhydrite and halite **are present**. If a map unit was interpreted as dominated by evaporites,
287 it was classified as E, regardless of other mentioned rocks. This implies that E class may additionally contain, e.g., carbonates.
- 288 • **Glacial drift (Gd):** include moraines and other related deposits.
- 289 • **Intrusive rocks (Ir):** acid (granites, quartz-diorites, quartz-monzonites), intermediate (diorite, monzonite, syenite),
290 and basic (gabbros and peridotites) plutonics. Ophiolite structures are included into basic plutonic except for basalt (Lb class)
291 and serpentinite (Sr class).
- 292 • **Lakes and Ice (Li):** lakes, rivers, ice and glaciers on some Alpine mountains. However, the coverage is not
293 representative for a lake or ice extent, as the priority of this map is on lithology.
- 294 • **Lavas and basalts (Lb):** volcanic rocks including acid (rhyolites, trachytes or dacites), intermediate (andesites) and
295 basic (basalt-type rocks, tephrites, tholeites and lamprophyres) volcanics.
- 296 • **Marlstone (M):** includes mostly marly rocks with a composition ranging from calcareous marls to clayey limestones.
297 Typically, it contains marly sediments of cartographic importance associated with Carbonatic rocks (Cr) or Siliciclastic
298 sedimentary rocks (Ssr).
- 299 • **Mass wasting material (Mw):** include landslides.
- 300 • **Mixed sedimentary rocks (SM):** sediments where carbonate is mentioned but not dominant. The class encompasses
301 mixed sedimentary rocks that are usually a combination of different rock types (e.g., interlayered sandstone and limestone, or
302 shaley marl with interlayered subordinated calcilutite beds or radiolarite). Mixed pelagic sediments as well as calcareous
303 turbidites are included in the SM class.
- 304 • **Non-schistose metamorphic rocks (Nsr):** metamorphics where schistose fabric can be present but not dominant. It
305 contains gneiss, amphibolite, quartzite, meta-conglomerate, and marble.
- 306 • **Pyroclastic rocks (Pr):** sediments of volcanic origin. Typical pyroclastics are tuff, volcanic breccias, ash, slag,
307 pozzolane, pumice.
- 308 • **Schistose metamorphic rocks (Sr):** 'broad' lithological class that encompasses a wide variety of rocks from **phyllite**
309 to schist, including association of schist and paragneiss. Ophiolite derived rocks that show a certain degree of metamorphism
310 and schistosity (e.g. Serpentinite) are included in this class
- 311 • **Siliciclastic sedimentary rocks (Ssr):** sandstone, mudstone and greywacke. Where carbonate was named in the rock
312 description of the mapped unit, the lithological classes Cr or SM was used, so siliciclastic sedimentary rocks are without
313 mapped carbonate influence. Note that in some cases the carbonate presence (e.g., as matrix) may not be named in the rock
314 description, and siliciclastic sediments may still contain carbonate in nature.

315 • **Unconsolidated clastic rock (Ucr):** young, not yet consolidated and/or weathered sediments, usually of Neogene
 316 and Quaternary age. It comprises all grain sizes with a heterogeneous origin loosely arranged and not cemented together.
 317 Examples of unconsolidated sediments are clay soil, sand, not cemented breccia, loose debris and conglomerate.
 318 Significant regional differences in the distribution of lithologies exist (Figure 6a,b,c, Table 4).



319

320 **Figure 6:** (a) Physical map of Italy subdivided into 18 physiographic regions; (b) Geographical distribution of the identified 19 lithological
 321 classes in the 18 physiographic regions of Italy (see Table 4 for spelling out the acronyms); (c) Percentage distribution of the 19 lithological
 322 classes in each physiographic region; (d) Polygons density (black symbols) and number of unique description (blue symbols) in each
 323 physiographic region considering the original data (points) and the LMI (arrow tips), and taking into account the years of publication of the
 324 geological sheets; (e) Legend. See Figure 5 for the extended lithological legend.

325

327 With the exception of flat and low-lying areas of Italy, where alluvial deposits and loose clastic deposits dominate (e.g. Po
328 Plain, PP), the map shows a high regional lithological variability. In the Western Alps (WAL) metamorphic rocks dominate
329 while in the Eastern Alps (EAL) carbonate rocks prevail. Intermediate percentages are recorded in the Central Alps (CAL),
330 where the metamorphic rocks to the N-NW and the sedimentary rocks to the S-SE are separated by an important tectonic
331 lineament. The northern Apennines (NAP) are mainly composed of siliciclastic rocks, and subordinately of chaotic and mixed
332 sedimentary rocks, while the central Apennines (CAP) mainly consist of carbonate rocks. Intermediate percentages of
333 carbonate rocks, mixed and chaotic sedimentary rocks, and siliciclastic deposits are found in the North Internal Apennines
334 (NIAP), in the Southern Apennines (SEAP) and in the Western Sicily (WS). In WS significant percentages of evaporites are
335 also recorded. In the Central and South Eastern Apennines (CEAP and SEAP), high percentages of unconsolidated and
336 consolidated clastic rocks are present, while carbonate rocks dominate the lithology of the Gargano and the Murge Foreland
337 (GF and MF). The similarity between the most represented lithological classes in the Calabro-Peloritano Arc (CPA) and
338 Sardinian Block (SB) is evident, although schistose rocks prevail in CPA while intrusive rocks prevail in SB. Volcanic rocks
339 are extensively represented in the Central and Southern Magmatic Province (CMP and SMP), in the Eastern Sicily (ES), in the
340 Sardinian Block (SB), and subordinately in the Eastern Alps (EAL).

341 Significant regional differences in the representation of lithologies also exist (Figure 6d). In the original geological dataset, the
342 number of polygons per squared kilometres (black points in Figure 6d) used to represent the lithological variability is strongly
343 heterogeneous across Italy, and is proportional to the geo-lithological complexity of each physiographic region. For instance,
344 the Alpine regions (EAL, CAL, WA), which are characterized by a complex geological architecture and by a very high
345 lithological variability, display the higher polygon density, with values between 1.7 e 2.4 polygons/km². On the other hand,
346 the Po Plain (PP) records the lowest polygons density, with 0,2 polygons per square kilometre, being characterized by a quite
347 monotonous surface geology, almost totally represented by alluvial deposits. Accordingly, in the Apennine regions, which are
348 (in general) geologically less complex than the Alpine regions, the average polygon density is just over 1 (NAP, NIAP, CAP,
349 SMP, SAP) with a maximum of 1,7 in the Central Magmatic Province (CMP) and a minimum of 0,3 in the south-eastern
350 regions of the foredeep (SEAP) and foreland (MF) domains.

351 The reclassification of the original geological dataset in the LMI classes determined the merging of adjacent polygons exposing
352 rock unit included in the same lithological class. The process resulted in a drop of the number of polygons in each physiographic
353 region, passing from the original data set to the LMI, which is indicated by the length of the black arrows in Figure 6d.
354 Importantly, the reduction of the number of polygons does not change the relative regional variability of the polygon density.
355 This means that the simplification introduced by our reclassification does not impact the regional difference in the
356 representation of the lithology.

357 In Figure 6d, the indicator of polygon density (in black) is flanked by an analogue indicator (in blue) displaying the count of
358 the unique descriptions used within each physiographic region, both in the original data set (blue points) and in the reclassified
359 LMI (blue arrow tips). The number of unique descriptions is generally proportional to the polygon density, but cases of
360 exceptionally high number of unique descriptions (e.g. PP, NAP, NIAP, SAP) are common. Primarily, this is the effect of
361 individual geologists or working groups using several local names to define the same rock unit, thus increasing the number of
362 unique descriptions.

363 Finally, Figure 6d shows that regional differences in the representation of lithologies may be also related to the different years
364 of publication of the geological sheets encompassed in each region. Figure 6d shows that: i) the geological sheets encompassed
365 in the Alpine region have been surveyed in the 1901-1940 (EAL, WAL) and 1961-1989 (CAL) **time intervals**; ii) almost all
366 the geological sheets encompassed in the regions of the Italian Peninsula (PP, NAP, NIAP, CEAP, CAP, CMP, SMP, SAP,
367 SEAP, GF, MF) have been surveyed in the 1961-1989 **time interval**, as those of the Sardinian Block (SB); iii) the geological
368 sheets of Western Sicily (WS) Eastern Sicily (ES) and Calabro Peloritano Arc (CPA) have been surveyed in the 1884-1900
369 **time interval**. While it is not clear whether the publication year of the geological sheets plays or not a role in controlling the
370 polygon density in the Alpine regions, the impact of the different years of publications in the representation of the regional
371 lithological variability is dramatic comparing CPA and SB. In fact, despite a similar lithological composition (Figure 6c) and
372 a pre-Alpine common geological history (Alvarez and Shimabukuro, 2009), CPA and SB are characterized by a very different
373 density of polygons (0,3 polygons/km² for CPA, and 1,3 for SB), due to strong differences in drafting geological sheets
374 published almost 100 years apart from each other.

375 **5 Discussions**

376 The main challenge in developing a categorized lithological map lies in balancing accuracy and complexity and still properly
377 representing the diversity of lithological variables using a limited yet reasonable number of classes, to ensure ready
378 interpretation and applicability of the map. We maintain that the 19 classes defined here allow to optimize the use of the map
379 for several applications, with a focus on landslides modelling. Despite the specific goals of this work, we applied a
380 classification that can be reconciled with the ones adopted in global lithological databases (Table 1; Hartmann et al., 2012;
381 Geological Survey of Canada, 1995), emphasizing the dominant rock types. Furthermore, information on the physical
382 characteristics of the dominant rock types available in the original geological legend were used to define specific lithological
383 classes.

384 For example, metamorphic rocks were split into two broad classes considering the dominant presence of schistose or not
385 schistose rocks, hence according to expected - or not expected - pervasive planar anisotropies within the rock bodies. Similarly,
386 the classes of consolidated and unconsolidated clastic sediments, in our map, consist of two separate classes, according to their
387 expected different geotechnical behaviour. In both cases, differences in physical features (e.g. schistose/non-schistose,

388 consolidated/unconsolidated) may impact landslide susceptibility of genetically similar rocks (Bucci et al., 2016b), hence
389 justifying the need of these lithological classes for our scope.

390 We also included the class Marlstone, quite unusual for generalized lithological characterization at national scale. The need
391 for this class arises from the systematic occurrence of significant marls interbeds within carbonate or siliciclastic rocks, whose
392 representation highlights the cartographic detail of the map. Moreover, it is widely recognized that marls intercalations
393 represent important geo-hydrological and mechanical discontinuities within rocks bodies (e.g. see Peacock et al., 2017), often
394 promoting landslide phenomena (Guzzetti et al., 1996), which is a relevant issue for our purpose. Since our map is designed
395 to be used for landslides studies and modelling, we also decided to maintain the class “landslides”, although it covers only
396 0,1% of the Italian territory. We are aware that this percentage value is strongly underestimated. The Inventory of Italian
397 Landslides (Trigila et al., 2010), still incomplete, counts over 620,000 landslides covering a total area equal to 7.9% of the
398 Italian territory, and occurrence of the different types of landslides gives rise to very different patterns of landslide
399 susceptibility, consistently with the diverse lithological formations (Lombardo et al., 2021). However, we acknowledge that
400 the large difference in percentage values stems from the fact that many efforts in landslide mapping have been made in recent
401 decades, when the 277 sheets of the geological map of Italy at 1: 100,000 scale were already published.

402 Despite the usage of very specific lithological classes helps a reliable classification of the rock types, the map is still subject
403 to uncertainty considering rock properties of some broad lithological classes. This is highlighted, for instance, by the
404 considerable amount of mixed limestone, marls and shale sediments (5%), including the Chaotic (2.2%) and the Mixed
405 sedimentary (2.8%) classes. Despite carbonate rocks and siliciclastic rocks behave differently for a large range of physical or
406 chemical properties (e.g., weathering processes, dissolution rates or aquifer characteristics), they occur often “mixed” in these
407 two geo-lithological classes, further undistinguishable at the scale of the used maps here.

408 An additional source of uncertainty remains at the boundaries of the geological sheets, where only discontinuities between
409 contiguous sheets longer than 1 km were resolved, with the exception of 58 segments over the entire national territory. Table
410 5 represents a contiguity matrix for these 58 segments. Table 5 reveals that 19 segments, 33% of the total, bound polygons
411 pertaining to the Al (Alluvial and marine deposits) class, which is the most represented lithological class at national scale,
412 covering the 25% of the entire national territory. The segments that bound lithological classes belonging to the same genetic
413 groups (metamorphic, magmatic, sedimentary) are 24, 10 of which separate lithological classes of the sedimentary substratum
414 from others belonging to sedimentary covers. Only 15 segments bound lithological classes belonging to different genetic
415 groups. Despite all these segments represent identical inconsistencies from a graphical point of view, their potential negative
416 local effects on the map reliability may be different from a lithological point of view. For instance, for landslide studies, we
417 can consider negligible the potential negative effects of unrealistic, linear lithological boundaries of polygons pertaining to the
418 Al class since they cover (almost) only flat areas of fluvial, alluvial and coastal plain, where landslides are unexpected.

419
420

I level classification →		Metamorphic		Magmatic			Sedimentary													
II level classification →		Metamorphic		Intrusion	Cover		Substratum					Undifferentiated Cover						Alluvial/Marine		
III level classification →		Sr	Nsr	Ir	Pr	Lb	Cr	M	SM	Cm	Ssr	E	Ucr	Ccr	Gd	Mw	Ad	Li	B	Al
Metamorphic	Sr	0	3	2	0	0	2	0	0	0	1	0	3	1	2	0	0	0	0	1
	Nsr	3	0	1	0	0	0	0	0	0	0	0	0	0	1	0	0	0	0	2
Magmatic	Ir	2	1	0	1	0	0	0	0	0	0	0	0	0	0	0	0	0	0	4
	Pr	0	0	1	0	0	0	0	0	0	0	0	1	0	1	0	0	0	0	1
	Lb	0	0	0	0	0	0	0	0	0	0	0	0	0	0	0	0	0	0	0
Sedimentary substratum	Cr	2	0	0	0	0	0	1	0	0	2	0	3	2	0	0	0	0	0	1
	M	0	0	0	0	0	1	0	0	0	3	0	0	0	0	0	0	0	0	1
	SM	0	0	0	0	0	0	0	0	0	0	0	1	0	0	0	0	0	0	0
	Cm	0	0	0	0	0	0	0	0	0	1	0	0	0	0	0	0	0	0	1
Undifferentiated sedimentary cover	Ssr	1	0	0	0	0	2	3	0	1	0	0	2	2	0	0	0	0	0	2
	E	0	0	0	0	0	0	0	0	0	0	0	0	0	0	0	0	0	0	1
	Ucr	3	0	0	1	0	3	0	1	0	2	0	0	3	0	0	0	0	0	0
	Ccr	1	0	0	0	0	2	0	0	0	2	0	3	0	0	0	0	0	0	2
	Gd	2	1	0	1	0	0	0	0	0	0	0	0	0	0	0	0	0	0	2
	Mw	0	0	0	0	0	0	0	0	0	0	0	0	0	0	0	0	0	0	0
	Ad	0	0	0	0	0	0	0	0	0	0	0	0	0	0	0	0	0	0	0
Alluvial/Marine	Li	0	0	0	0	0	0	0	0	0	0	0	0	0	0	0	0	0	0	0
	B	0	0	0	0	0	0	0	0	0	0	0	0	0	0	0	0	0	0	1
	Al	1	2	4	1	0	1	1	0	1	2	1	0	2	2	0	0	0	1	0
Total number →		15	7	8	4	0	11	5	1	2	13	1	13	10	6	0	0	0	1	19

421

422 **Table 5:** Contiguity matrix showing the number of the 58 N-S and E-W oriented straight segments longer than 1000 m which bounds each
423 lithological class.

424

425 On the other hand, critical differences remain between rocks pertaining to the same genetic group but characterized by different
426 physical properties (schistose/non schistose metamorphic rocks, consolidated/unconsolidated sedimentary clastic rocks).
427 Overall, we consider as resolved the inhomogeneity problems at the boundaries between adjacent geological sheets for
428 segments equal to or greater than 1000 meters, hence considering the remaining 58 segments longer than 1000 meters listed
429 in Table 1 as acceptable and/or negligible exceptions. Since in cartography the admissible error is traditionally assumed to be
430 1 mm, we maintain that, only along the boundaries of the geological sheets our map is formally correct at the 1:1,000,000
431 **scale**, while elsewhere the cartographic detail remains compatible with the 1:100,000 **scale**. Pushing harmonization operation
432 into more detail would require altering the original data, which is outside the scope of this work.

433 The design of the LMI allows for further corrections and inclusion of additional information, (*e.g.*, age information, tectonic
434 history, geotechnical properties, fine-coarse grain size ratio) in future versions, customizable for different usage, with expected
435 reduction of general and/or specific uncertainties. Additional information may be organized into more detailed classification
436 levels, although their compilation will require further efforts to collect data from local geo-lithological literature and site-
437 specific investigations.

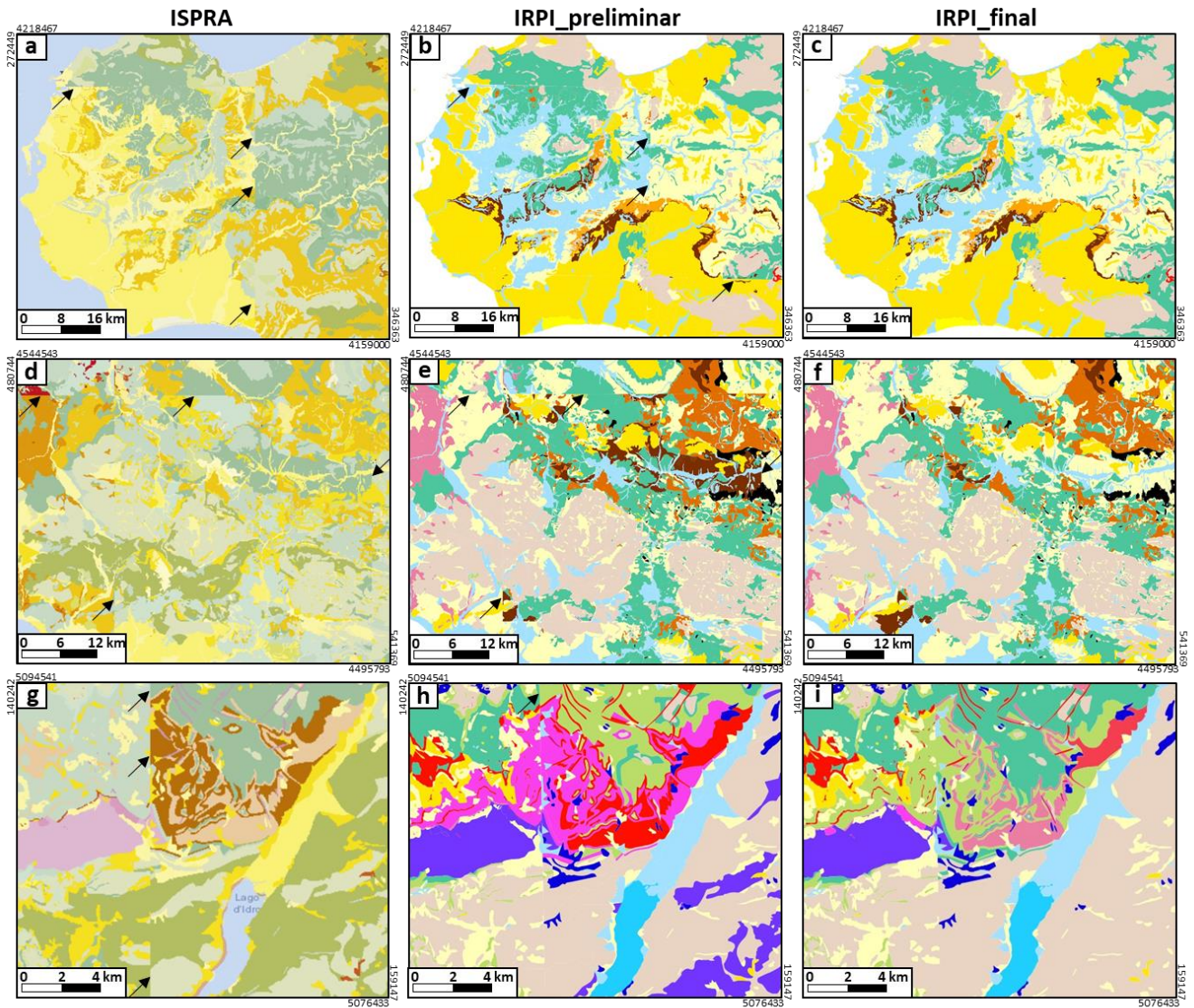
438 Since different purposes impose different generalization strategies, other lithological classifications of the Italian rocks are
439 possible, starting from the same source dataset. For instance, aiming at a seismic soil classification of Italy, Forte et al. (2019)
440 generalized the lithology of Italy using 20 classes, a number comparable to the 19 classes presented here. In Forte et al.
441 (2019)'s classification, a relevant distinction was based on the identification of geo-lithological complexes as geologic
442 bedrock, versus those representative of cover deposits, being the last category directly related to defined values of V_S (average
443 speed of propagation of shear waves), hence particularly relevant for their purpose. On the other hand, the most recent

444 lithological map of Italy provided by ISPRA as a web service is accompanied by a complex legend, articulated in 48 classes
445 aimed at describe age, genesis and chemical-physical characteristics of rocks, focusing on a comprehensive geological rock
446 characterization, without specific applicative purpose. It is evident that different classifications allow different possible usages
447 of the same original dataset, hence, at the same representation scale, different lithological characterizations can be more or less
448 suitable depending on the intended purpose.

449 Although the general rock composition of the Italian's surface is remarkably similar between the existing digital lithological
450 maps (Table 1, ID 5) the representation of the rock distribution varies largely between them, and have been greatly improved
451 in the present map, especially across geological sheets. Compared to smaller-scale maps (Compagnoni et al., 1976-1983), the
452 main improvements lays in a better representation of complex geological settings. Moreover, a better lithological
453 harmonization along the borders of the original geological sheets distinguishes our map from other maps at the same scale
454 (Servizio Geologico d'Italia, 2004). Figure 7 shows examples for Sicilia, Campania and Lombardia regions, highlighting the
455 general improvement of the map, regardless of the geographical location, geological and geomorphological settings. However,
456 a direct comparison of the maps is difficult due to the different legends (*e.g.* based on geological processes or lithology, or
457 mixing up processes and lithology).

458 Early versions of the LMI presented here were already used to validate terrain classification of Italy (Alvioli et al., 2020) and
459 to estimate soil parameters for physically based rockfall modelling along the Italian railway (Alvioli et al., 2021). Such versions
460 of the map included a few of the inconsistencies resolved in this work. We expect that a similar use of the map could be
461 extended to study and model other types of landslides in different lithological settings, both widespread in the landscape and
462 along specific infrastructure networks.

463



464

465 **Figure 7:** Comparison of two different classifications of the same source dataset for selected areas of Sicily (a, b, c), Campania (d, e, f) and
 466 Lombardia (g, h, i) regions. Examples from the lithological map of Italy according to ISPRA classification as visualized in vector form at
 467 the ISPRA website (Table 1, ID 5) are shown in (a), (d) and (g). For the same areas, the lithological map of Italy according to our own
 468 preliminar semi-automatic classification partially resolved the major inconsistencies along the boundaries of the geological sheets already
 469 present in (a), (d) and (g), even if critical boundaries still remains, see black arrows as reference; Most of the inconsistencies were resolved
 470 manually by expert analysis in the final version of our map (c, f, i) leading a substantial improvement of the lithological harmonization along
 471 the borders of the original geological sheets.

472

473

474 **6 Conclusions**

475 This paper described the first freely downloadable lithological map of Italy at **the** 1:100.000 scale, providing the distribution
476 of rock-attributes and rock-types of the Italian territory in digital format.

477 The LMI was assembled from 277 sheets of the Geological Map of Italy at **the** 1: 100,000 scale and distributed in digital vector
478 format through a REST service on the ISPRA website. For the purpose, the rock types associated with the 5.456 unique
479 geological descriptions in the source dataset were identified and translated into the 19 general classes defined here. Adjacent
480 polygons grouped within the same class were dissolved, reducing their number from the original 292,705 to the 180,503 in the
481 final product. Most of the work consisted with database queries, coupled with expert analysis of the location of the polygons
482 using the sheets available at **the** 1:50,000 **scale** (where present), and with any potentially useful information sought in regional
483 and local literature. Particular attention was paid to harmonize the lithological information at the **boundaries** of the original
484 geological sheets. A final technical validation allowed to detect and resolve residual problems, also related to inconsistencies
485 inherited from the source dataset, and guaranteed the overall quality of the work.

486 The LMI allows the assessment of national scale research questions at high resolution and thus helps to advance our knowledge
487 on the relationships between lithology and surface processes, including multiple geomorphological, geo-hydrological and
488 environmental issues. In addition, the resolution of the LMI highlights the differences in the lithological cover of the different
489 regions and sub-regions, hence facilitating the comparison of results of different regional studies (*e.g.*, susceptibility to
490 landslides and floods).

491 The map has limits and can be enhanced, in particular in local areas where geo-lithological descriptions in the source dataset
492 were not exhaustive and our knowledge is limited. Inclusion of more detailed regional maps or other relevant additional
493 information, *e.g.*, age, tectonic history, geotechnical properties, fine-coarse grain size ratio are out of the aim of this work, but
494 may be included in future versions. Aware of these and other potential and desirable future upgrades, we provided the LMI
495 with a very simple and open architecture, which allows more details or levels of information to be added and could thus be
496 developed further in accordance with specific scientific questions.

497 **7 Data availability**

498 The digital lithological Map of Italy at 1:100.000 is provided in the PANGAEA database.
499 <https://www.pangaea.de/tok/0ea29920145583a489026d832be5c94997d0235e> (Bucci et al. 2021).

500 **8 Contributions**

501 Francesco Bucci (FB), Michele Santangelo (MS), Lorenzo Fongo (LF), Mauro Cardinali (MC) and Ivan Marchesini (IM)
502 decided the classification system, performed multiscale comparative analysis, and drafted the final version of the lithological

503 map. Ivan Marchesini (IM) e Massimiliano Alvioli (MA) prepared the dataset and the script for the final classification. FB,
504 MS, LF, MC, IM and Laura Meelli (LM) compiled the Legend and designed the layout of the final map. FB, MS wrote the
505 text. LF, MC, IM, MA, LM reviewed and integrated the paper at several stages, IM supervised the research activity.

506 **9 Acknowledgements**

507 The work was partly carried out within the FRA.SI (Multi-scale integrated methodologies for seismically-induced landslides
508 risk zonation) project, of the National Research council of Italy (CNR).

509 **References**

- 510 Alvarez, W., Shimabukuro D.H.: The geological relationships between Sardinia and Calabria during Alpine and Hercynian
511 times. *Italian Journal of Geosciences*, 128, 2, 257–268. doi: <https://doi.org/10.3301/IJG.2009.128.2.257>, 2009.
- 512 Alvioli, M., Guzzetti, F., Marchesini, I.: Parameter-free delineation of slope units and terrain subdivision of Italy,
513 *Geomorphology*, 358, 107-124. <https://doi.org/10.1016/j.geomorph.2020.107124>, 2020.
- 514 Alvioli, M., Marchesini, I., Reichenbach, P., Rossi, M., Ardizzone, F., Fiorucci, F., Guzzetti, F.: Automatic delineation of
515 geomorphological slope units and their optimization for landslide susceptibility modelling, *Geosci. Model Dev.* 9,
516 3975–3991. <https://doi.org/10.5194/gmd-9-3975-2016>, 2016.
- 517 Alvioli, M., Santangelo, M., Fiorucci, F., Cardinali, M., Marchesini, I., Reichenbach, P., Rossi, M., Guzzetti, F., Peruccacci,
518 S.: Rockfall susceptibility and network-ranked susceptibility along the Italian railway. *Engineering Geology*, 2021 (in
519 press).
- 520 Amanti, M., Battaglini, L., Campo, V., Cipolloni, C., Congi, M.P., Conte, G., Delogu, D., Ventura, R., Zonetti, C.: The
521 Lithological map of Italy at 1:100.000 scale: An example of re-use of an existing paper geological map. In: 33rd
522 International Geological Conference, IEI02310L - 6-14th August, Oslo (Norway), 2008.
- 523 Amanti, M., Battaglini, L., Campo, V., Cipolloni, C., Congi, M.P., Conte, G., Delogu, D., Ventura, R., Zonetti, C.: La carta
524 litologica d'italia alla scala 1:100.000. *Atti della 11a Conferenza Nazionale ASITA, Centro Congressi Lingotto, Torino,*
525 *6–9 Novembre 2007*, <http://atti.asita.it/Asita2007/Pdf/119.pdf>, 2007.
- 526 Amodio Morelli, L., Bonardi, G., Colonna, V., Dietrich, D., Giunta G., Liguori, V., Lorenzoni, S., Paglianico, A., Perrone, V.,
527 Piccarreta, G., Russo, M., Scandone, P., Zanettin, E., Zuppetta, A.: L'arco Calabro Peloritano nell'Orogene
528 Appenninico-Magrebide, *Memorie della Società Geologica Italiana*, 17, 1-60, 1976.
- 529 Asch, K.: The 1:5 million international geological map of Europe and adjacent areas. *Bundesanstalt für Geowissenschaften*
530 *und Rohstoffe, Commission of the Geological Map of the World, Subcommittee for Europe. BGR, Hannover, 2005.*

- 531 Bentivenga, M., Coltorti, M., Prosser, G., Tavarnelli, E.: Deformazioni distensive recenti nell'entroterra del Golfo di Taranto:
532 implicazioni per la realizzazione di un deposito geologico per scorie nucleari nei pressi di Scanzano Jonico (Basilicata),
533 Boll. Soc. Geol. It., 123, 3, 391-404, 2004.
- 534 Boni, C.F., Bono, P., Funicello, R., Parotto, M., Praturlon, A., Fanelli, M.: Carta delle manifestazioni termali e dei complessi
535 idrogeologici, scala 1:1.000.000. In: Contributo alla conoscenza delle risorse geotermiche del territorio italiano. CNR,
536 Progetto Finalizzato Energetica, Sottoprogetto Energia Geotermica, Roma, 1984.
- 537 Bonomo, R., Capotorti, F., D'Ambrogi, C., Di Stefano, R., Graziano, R., Martarelli, L., Pampaloni, M.L., Pantaloni, M., Ricci,
538 V., Compagnoni, B., Galluzzo, F., Tacchia, D., Masella, G., Pannuti, V., Ventura, R., Vitale, V.: Carta geologica d'Italia
539 alla scala 1:1.250.000, Serv. Geol. d'It., APAT, Roma, 2005.
- 540 Bortolotti, V., Fazzuoli, M., Pandelli, E., Principi, G., Babbini, A., Corti, S.: Geology of Central and Eastern Elba Island, Italy,
541 Ofioliti, 26(2): 97-150, 2001.
- 542 Brogi, A., Liotta, D.: Fluid flow paths in fossil and active geothermal fields: the Plio-Pleistocene Boccheggiano-Montieri and
543 the Larderello areas, Geological Field Trips of the Italian Geological Society, vol. 3(2.2), ISSN: 2038- 4947,
544 doi:10.3301/GFT.2011.03, 2011.
- 545 Brozzetti, F.: Geological map (1: 25.000 scale) of the Northern Umbria Preapennines in the M:S:M: Tiberina area (Umbria
546 Italy). Boll. Soc. Geol. It, 126, 511-529, 2007.
- 547 Bucci, F., Novellino, R., Guglielmi, P., Prosser, G., & Tavarnelli, E. (2012). Geological map of the northeastern sector of the
548 high Agri Valley, Southern Apennines (Basilicata, Italy). Journal of Maps, 8, 282–292.
549 <https://doi.org/10.1080/17445647.2012.722403>
- 550 Bucci, F., Novellino, R., Tavarnelli, E., Prosser, G., Guzzetti, F., Cardinali, M., Gueguen, E., Guglielmi, P., Adurno, I.: Frontal
551 collapse during thrust propagation in mountain belts: a case study in the Lucania Apennines, Southern Italy, J. Geol.
552 Soc. 171, 571–581, <https://doi.org/10.1144/jgs2013-103>, 2014.
- 553 Bucci, F., Mirabella, F., Santangelo, M., Cardinali, M., Guzzetti, F.: Photo-geology of the Montefalco Quaternary Basin,
554 Umbria, Central Italy, Journal of Maps 12:314–322, <https://doi.org/10.1080/17445647.2016.1210042>, 2016a.
- 555 Bucci, F., Santangelo, M., Cardinali, M., Fiorucci, F., Guzzetti, F.: Landslide distribution and size in response to Quaternary
556 fault activity: the Peloritani Range, NE Sicily, Italy, Earth Surf. Process. Landf. 41, 711–720,
557 <https://doi.org/10.1002/esp.3898>, 2016b.
- 558 Bucci, F., Tavarnelli, E., Novellino, R., Palladino, G., Guglielmi, P., Laurita, S., Prosser, G., Bentivenga, M.: The History of
559 the Southern Apennines of Italy Preserved in the Geosites Along a Geological Itinerary in the High Agri Valley,
560 Geoheritage 11, 1489–1508, <https://doi.org/10.1007/s12371-019-00385-y>, 2019.
- 561 Bucci, F., Novellino, R., Guglielmi, P., Tavarnelli, E.: Growth and dissection of a fold and thrust belt: the geological record
562 of the High Agri Valley, Italy. J. Maps 16, 245–256, <https://doi.org/10.1080/17445647.2020.1737254>, 2020.

563 Bucci, F., Santangelo, M., Fongo, L., Alvioli, M., Cardinali, M., Melelli, L., Marchesini, I.: A new digital lithological Map of
564 Italy at 1:100.000 scale. PANGAEA, <https://doi.pangaea.de/10.1594/PANGAEA.935673> (dataset in review), 2021.

565 Calamita, F., Esestime, P., Paltrinieri, W., Scisciani, V., Tavarnelli, E. (2009). Structural inheritance of pre- and synorogenic
566 normal faults on the arcuate geometry of Pliocene-Quaternary thrusts: Examples from the Central and Southern
567 Apennine Chain. *Italian Journal of Geosciences (Boll. Soc. Geol. It.)*, 128, 2, 381-394
568 (DOI:10.3301/IJG.2009.128.2.381)

569 Campobasso, C., Salvati, L., Vita, L. Eds.: Evoluzione dei bacini neogenici e loro rapporti con il magmatismo plio-quaternario
570 dell'area tosco-laziale (Pisa, 1991), Mem. Descr. Carta Geol. d'It., 49, pp. 375, Ser. Geol. d'It., Roma, 1994.

571 Carmignani, L., Conti, P., Cornamusini, G., Pirro, A.: Geological map of Tuscany (Italy), *J. Maps* 9, 487-497,
572 <https://doi.org/10.1080/17445647.2013.820154>, 2013.

573 Carmignani, L.: Geologia della Sardegna. Note illustrative della Carta Geologica della Sardegna a scala 1:200.000. Mem.
574 Descr. Carta Geol. d'It., 60: pp. 283, Serv. Geol. d'It., Roma, 2001.

575 Catanzariti, R., Ottria, G., Cerrina Feroni, A.: Carta geologico-strutturale dell'Appennino Emiliano-Romagnolo. Scala
576 1:250.000. RER - Servizio Geologico, Sismico e dei Suoli; CNR - Istituto di Geoscienze e Georisorse, Pisa, 2002.

577 Celico, P.B., De Vita, P., Monacelli, G., Scalise, A.R., Tranfaglia, G.: Carta idrogeologica dell'Italia Meridionale, scala
578 1:250.000. ISPRA, Roma, 2005.

579 Centamore, E., Panbianchi, G., Deiana, G., Calamita, F., Cello, G., Dramis, F., Gentili, B., Nanni, T.: Ambiente fisico delle
580 Marche. Geologia, Geomorfologia, Idrogeologia alla scala 1:100.000. Regione Marche, 1991.

581 Centamore, E., Rossi, D., Tavarnelli, E. (2009). Geometry and kinematics of Triassic-to-Recent structures in the
582 Northern-Central Apennines: a review and an original working hypothesis. *Italian Journal of Geosciences (Boll. Soc.
583 Geol. It.)*, 128, 2, 419-432 (DOI: 10.3301/IJG.2009.128.2.419).

584 Chiarini, E., D'Orefice, M., Graciotti, R.: Le unità stratigrafiche di riferimento nella rappresentazione cartografica dei depositi
585 plio-quaternari continentali nel Progetto CARG. Esempi: Arco alpino, Pianura Padana e Sardegna. *Il Quaternario*, 21,
586 1A, 51-56, 2008.

587 Cipolloni, C., Pantaloni, M., Ventura, R., Vitale, V., Tacchia, D.: The GEO1MDB: the database of the 1:1,000,000 scale
588 geological map of Italy. In: 6th EUREGEO Proceeding, 1: 218-221, 2009.

589 Compagnoni, B.: La Carta geologica d'Italia, alla scala 1:1.000.000. Mem. Descr. Carta Geol. It., 71, 207-212, 2004.

590 Compagnoni, B., Damiani, A.V., Valletta, M.: Carta geologica d'Italia alla scala 1:500.000. In 5 fogli e note illustrative,
591 Servizio Geologico d'Italia, Roma, 1976-1983.

592 Consiglio Nazionale delle Ricerche: Structural model of Italy and gravity map. *Quaderni della Ricerca Scientifica*, 114, 3,
593 1990.

594 Console, F., Pantaloni, M., Petti, F.M., Tacchia, D.: La cartografia del Servizio geologico d'Italia = The Geological survey of
595 Italy mapping, ISBN:978-88-9311-052-5, 2017.

596 Conti, P., Cornamusini, G., Carmignani, L.: An outline of the geology of the Northern Apennines (Italy), with geological map
597 at 1:250,000 scale, Ital. J. Geosci. 139, 149–194, <https://doi.org/10.3301/IJG.2019.25>, 2020.

598 Corpo Reale delle Miniere: Carta mineraria d'Italia. Scala 1:500.000, Roma, 1926-1935.

599 Coulthard, T.J.: Landscape evolution models: A software review, Hydrol. Processes, 15, 1, 165–173, doi:10.1002/hyp.426,
600 2001.

601 D'Ambrogio, C., Scrocca, D., Pantaloni, M., Valeri, V., Doglioni, C.: Exploring Italian geological data in 3D. In: M.
602 BELTRANDO, A. PECCERILLO, M. MATTEI, S. CONTICELLI & C. DOGLIONI: The Geology of Italy. Journal
603 of the Virtual Explorer, 36, paper 33. doi:10.3809/jvirtex.2010.00256, 2010.

604 De Graaf, I.E.M., Van Beek, R.L.P.H., Gleeson, T., Moosdorf, N., Schmitz, O., Sutanudjaja, E.H., Bierkens, M.F.P.: A global-
605 scale two-layer transient groundwater model: Development and application to groundwater depletion. Adv. Water
606 Resour. 102, 53–67. <https://doi.org/10.1016/j.advwatres.2017.01.011>, 2017.

607 De Rita D., Fabbrini, M., Cimarelli, C. (2004) - Evoluzione pleistocenica del margine tirrenico dell'Italia centrale tra
608 eustatismo, vulcanismo e tettonica. Il Quaternario, 17(2): 523-536.

609 De Sousa, L.M., Poggio, L., Batjes, N.H., Heuvelink, G.B.M., Kempen, B., Riberio, E., Rossiter, D., 2020. SoilGrids 2.0:
610 producing quality-assessed soil information for the globe. SOIL Discuss. 1–37. <https://doi.org/10.5194/soil-2020-65>

611 Delogu, D., Campo, V., Cipolloni, C., Congi, M.P., Falcetti, S., Moretti, P. Pampaloni, M. L., Pantaloni, M., Roma, M.,
612 Ventura, R.: Il Portale del Servizio Geologico d'Italia: uno strumento al servizio dei geologi professionisti. Professione
613 Geologo, 32, 4, 24-27, 2012.

614 Donnini, M., Marchesini, I., Zucchini, A., 2020a. Geo-LiM: a new geo-lithological map for Central Europe (Germany, France,
615 Switzerland, Austria, Slovenia, and Northern Italy) as a tool for the estimation of atmospheric CO₂ consumption. J.
616 Maps 16, 43–55. <https://doi.org/10.1080/17445647.2019.1692082>

617 Donnini, M., Marchesini, I., Zucchini, A., 2020b. A new Alpine geo-lithological map (Alpine-Geo-LiM) and global carbon
618 cycle implications. GSA Bull. 132, 2004–2022. <https://doi.org/10.1130/B35236.1>

619 Dürr, H.H., Meybeck, M., Dürr, S.H., 2005. Lithologic composition of the Earth's continental surfaces derived from a new
620 digital map emphasizing riverine material transfer. Glob. Biogeochem. Cycles 19, n/a-n/a.
621 <https://doi.org/10.1029/2005GB002515>

622 Forte, G., Chioccarelli, E., De Falco, M., Cito, P., Santo, A., Iervolino, I., 2019. Seismic soil classification of Italy based on
623 surface geology and shear-wave velocity measurements. Soil Dyn. Earthq. Eng. 122, 79–93.
624 <https://doi.org/10.1016/j.soildyn.2019.04.002>

625 Ge.Mi.Na. (1962). Ligniti e torbe dell'Italia continentale. Geomineraria nazionale, 1–319

- 626 Geological Survey of Canada, Open File 2915d, doi:10.4095/195142, 1995, [https://mrddata.usgs.gov/geology/world/map-](https://mrddata.usgs.gov/geology/world/map-us.html#home)
627 [us.html#home](https://mrddata.usgs.gov/geology/world/map-us.html#home) (access date 2021/05/07)
- 628 Giannandrea, P., La Volpe, L., Principe, C., Schiattarella, M. (2006) - Carta geologica del Monte Vulture. Scala 1:25.000. In:
629 PRINCIPE C., La geologia del Monte Vulture, CNR, Regione Basilicata. pp. 217.
- 630 Giardino, M. & Fioraso, G. (1998) - Cartografia geologica delle formazioni superficiali in aree di catena montuosa: il
631 rilevamento del F. "Bardonecchia" nell'ambito del progetto CARG. Mem. Sci. Geol., 50: 133-153
- 632 Gibbs, M.T., Kump, L.R., 1994. Global chemical erosion during the Last Glacial Maximum and the present: Sensitivity to
633 changes in lithology and hydrology. *Paleoceanography* 9, 529–543. <https://doi.org/10.1029/94PA01009>
- 634 Girotti, O. & Mancini, M. (2003) - Plio-Pleistocene stratigraphy and relations between marine and non-marine successions in
635 the middle valley of the Tiber river (Latium, Umbria). *Il Quaternario, Italian Journal of Quaternary Sciences*, 16 (1 bis):
636 89-106.
- 637 Giustini, F., Ciotoli, G., Rinaldini, A., Ruggiero, L., Voltaggio, M.: Mapping the geogenic radon potential and radon risk by
638 using Empirical Bayesian Kriging regression: A case study from a volcanic area of central Italy, *Science of The Total*
639 *Environment*, 661, 449-464, <https://doi.org/10.1016/j.scitotenv.2019.01.146>, 2019.
- 640 Gleeson, T., Smith, L., Moosdorf, N., Hartmann, J., Dürr, H. H., Manning, A. H., van Beek, L. P. H., and Jellinek, A. M.
641 (2011), Mapping permeability over the surface of the Earth, *Geophys. Res. Lett.*, 38, L02401,
642 doi:10.1029/2010GL045565.
- 643 Gueguen, E., Tavarnelli, E., Renda, P., Tramutoli, M. (2010). The southern Tyrrhenian Sea margin: an example of lithospheric
644 scale strike-slip duplex. *Italian Journal of Geosciences (Boll. Soc. Geol. It.)*, 129, 3, 496-505 (DOI:
645 10.3301/IJG.2010.15).
- 646 Guzzetti, F., Cardinali, M., Reichenbach, P. (1996). The influence of structural setting and lithology on landslide type and
647 pattern. *Environmental and Engineering Geosciences*, 2, 531–555. doi:10.2113/gseegeosci.ii.4.531
- 648 Han, L., Fuqiang, L., Zheng, D., Weixu, X. (2018). A lithology identification method for continental shale oil reservoir based
649 on BP neural network. *Journal of Geophysics and Engineering*, 15(3), 895–908. [https://doi.org/10.1088/1742-](https://doi.org/10.1088/1742-2140/aaa4db)
650 [2140/aaa4db](https://doi.org/10.1088/1742-2140/aaa4db)
- 651 Hartmann, J., N. Jansen, H. H. Dürr, A. Harashima, K. Okubo, and S. Kempe (2010), Predicting riverine dissolved silica fluxes
652 to coastal zones from a hyperactive region and analysis of their first order controls, *Int. J. Earth Sci.*, 99 (1), 207–230,
653 doi:10.1007/s00531-008-0381-5
- 654 Hartmann, J., Dürr, H.H., Moosdorf, N., Meybeck, M., Kempe, S., 2012. The geochemical composition of the terrestrial
655 surface (without soils) and comparison with the upper continental crust. *Int. J. Earth Sci.* 101, 365–376.
656 <https://doi.org/10.1007/s00531-010-0635-x>

657 Hartmann, J., Moosdorf, N., 2012. The new global lithological map database GLiM: A representation of rock properties at the
658 Earth surface: TECHNICAL BRIEF. *Geochem. Geophys. Geosystems* 13. <https://doi.org/10.1029/2012GC004370>

659 Horton, J.D., 2017, The State Geologic Map Compilation (SGMC) geodatabase of the conterminous United States (ver. 1.1,
660 August 2017): U.S. Geological Survey data release, <https://doi.org/10.5066/F7WH2N65>.

661 Ispra & Parco Nazionale del Cilento, Vallo di Diano e Alburni (2013) - Carta geologica con elementi tematici e carta dei
662 paesaggi sottomarini del Parco Nazionale del Cilento, Vallo di Diano e Alburni (European and Global Geopark).
663 Salerno. [http://www.isprambiente.gov.it/it/progetti/suolo-eterritorio-1/carta-geologica-del-parco-del-cilento-vallo-di-](http://www.isprambiente.gov.it/it/progetti/suolo-eterritorio-1/carta-geologica-del-parco-del-cilento-vallo-di-diano-e-degli-alburni)
664 [diano-e-degli-alburni](http://www.isprambiente.gov.it/it/progetti/suolo-eterritorio-1/carta-geologica-del-parco-del-cilento-vallo-di-diano-e-degli-alburni)

665 Lentini, F. & Carbone, S. Eds. (2014) - *Geologia della Sicilia. Mem. Descr. Carta Geol. d'It.*, 95: pp. 413, Serv. Geol. d'It.,
666 Roma

667 Lombardo, L., Loche, M., Marchesini, I., Alvioli, M., Bakka, H. (2021). A strategy to obtain statistically significant landslide
668 susceptibility maps from a spatially unbalanced, nation-wide inventory in Italy. Submitted for publication.

669 Lorenzo-Lacruz, J., Garcia, C., Morán-Tejeda, E., 2017. Groundwater level responses to precipitation variability in
670 Mediterranean insular aquifers. *J. Hydrol.* 552, 516–531. <https://doi.org/10.1016/j.jhydrol.2017.07.011>

671 Marchesini, I., Cencetti, C., & De Rosa, P., 2009. A preliminary method for the evaluation of the landslides volume at a
672 regional scale. *GeoInformatica*, 13(3), 277–289. <https://doi.org/10.1007/s10707-008-0060-5>

673 Marchesini, I., Mergili, M., Rossi, M., Santangelo, M., Cardinali, M., Ardizzone, F., Fiorucci, F., Schneider-Muntau, B., Fellin,
674 W., & Guzzetti, F., 2014. A GIS Approach to Analysis of Deep-Seated Slope Stability in Complex Geology. In K.
675 Sassa, P. Canuti, & Y. Yin (Eds.), *Landslide Science for a Safer Geoenvironment* (pp. 483–489). Springer International
676 Publishing. https://doi.org/10.1007/978-3-319-05050-8_75

677 Mergili, M., Marchesini, I., Rossi, M., Guzzetti, F., & Fellin, W., 2014a. Spatially distributed three-dimensional slope stability
678 modelling in a raster GIS. *Geomorphology*, 206, 178–195. <https://doi.org/10.1016/j.geomorph.2013.10.008>

679 Mergili, M., Marchesini, I., Alvioli, M., Metz, M., Schneider-Muntau, B., Rossi, M., Guzzetti, F., 2014b. A strategy for GIS-
680 based 3-D slope stability modelling over large areas. *Geosci. Model Dev.* 7, 2969–2982. [https://doi.org/10.5194/gmd-](https://doi.org/10.5194/gmd-7-2969-2014)
681 [7-2969-2014](https://doi.org/10.5194/gmd-7-2969-2014)

682 Ministero dei Lavori Pubblici, Ufficio Idrografico, Sezione Geologica (1948) - *Carta Geologica d'Italia alla scala 1:100.000 –*
683 *F. 35 Riva. Firenze.*

684 Mirabella, F., Bucci, F., Santangelo, M., Cardinali, M., Caielli, G., De Franco, R., Guzzetti, F., & Barchi, M. R. (2018).
685 Alluvial fan shifts and stream captures driven by extensional tectonics in central Italy. *Journal of the Geological Society*,
686 175, 788–805. <https://doi.org/10.1144/jgs2017-138>.

687 Mori, F., Mendicelli, A., Moscatelli, M., Romagnoli, G., Peronace, E., Naso, G., 2020. A new Vs30 map for Italy based on the
688 seismic microzonation dataset. *Eng. Geol.* 275, 105745. <https://doi.org/10.1016/j.enggeo.2020.105745>

689 Novellino, R., Bucci, F., Tavarnelli, E., 2021. Structural investigation of background features and normal faults affecting the
690 Calcarei con Selce Formation, Southern Apennines, Italy. *Ital. J. Geosci.* 140, 1–21. <https://doi.org/10.3301/ijg.2020.31>
691 Onegeology: <http://www.onegeology.org/portal/home.html> (access date 2021/05/07)

692 Pantaloni, M. (2011) - La Carta geologica d'Italia alla scala 1:1.000.000: una pietra miliare nel percorso della conoscenza
693 geologica. *Geologia Tecnica & Ambientale*, 2-3(11): 88-99

694 Patacca, E., Scandone, P., Bellatalla, M., Perilli, N., Santini, U. (1991) - La zona di giunzione tra l'arco Appennino
695 settentrionale e l'arco Appennino meridionale nell'Abruzzo e nel Molise. *Studi Geol. Camerti*, Vol. Spec. 2: 417-441.

696 Peacock, D.C.P., Anderson, M.W., Rotevatn, A., Sanderson, D.J., Tavarnelli, E. (2017). The interdisciplinary use of
697 “overpressure”. *Journal of Volcanology and Geothermal Research*, 341, 1-5.

698 Piana, F., Fioraso, G., Irace, A., Mosca, P., d'Atri, A., Barale, L., Falletti, P., Monegato, G., Morelli, M., Tallone, S., Vigna,
699 G.B., 2017. Geology of Piemonte region (NW Italy, Alps–Apennines interference zone). *J. Maps* 13, 395–405.
700 <https://doi.org/10.1080/17445647.2017.1316218>

701 Prosser, G. (2000) The development of the North Giudicarie fault zone (Insubric line, Northern Italy). *Journal of Geodynamics*,
702 30, 1-2, 229-250

703 R. Ufficio Geologico (1884a) - Carta Geologica d'Italia alla scala 1:100.000 – F. 248 Trapani. Roma.

704 R. Ufficio Geologico (1884b) - Carta Geologica d'Italia alla scala 1:100.000 – F. 249 Palermo. Roma.

705 R. Ufficio Geologico (1884c) - Carta Geologica d'Italia alla scala 1:100.000 – F. 257 Castevetrano. Roma.

706 R. Ufficio Geologico (1884d) - Carta Geologica d'Italia alla scala 1:100.000 – F. 258 Corleone. Roma.

707 R. Ufficio Geologico (1884e) - Carta Geologica d'Italia alla scala 1:100.000 – F. 266 Sciacca. Roma.

708 R. Ufficio Geologico (1900) - Carta Geologica d'Italia alla scala 1:100.000 – F. 228 Cetraro. Roma.

709 Raia, S., Alvioli, M., Rossi, M., Baum, R.L., Godt, J.W., Guzzetti, F., 2014. Improving predictive power of physically based
710 rainfall-induced shallow landslide models: a probabilistic approach. *Geosci. Model Dev.* 7, 495–514.
711 <https://doi.org/10.5194/gmd-7-495-2014>

712 Reichenbach, P., Rossi, M., Malamud, B.D., Mihir, M., Guzzetti, F., 2018. A review of statistically-based landslide
713 susceptibility models. *Earth-Sci. Rev.* 180, 60–91. <https://doi.org/10.1016/j.earscirev.2018.03.001>

714 Roche, V., Bouchot, V., Beccaletto, L., Jolivet, L., Guillou-Frottier, L., Tuduri, J., Bozkurt, E., Oguz, K., Tokay, B., 2019.
715 Structural, lithological, and geodynamic controls on geothermal activity in the Menderes geothermal Province (Western
716 Anatolia, Turkey). *Int. J. Earth Sci.* 108, 301–328. <https://doi.org/10.1007/s00531-018-1655-1>

717 Ronchi, A., Cassinis, G., Durand, M., Fontana, D., Oggiano, G., Stefani, C., 2011. Stratigrafia e analisi di facies della
718 successione continentale permiana e triassica della Nurra: confronti con la Provenza e ricostruzione paleogeografica.
719 *Geol. Field Trips* 3, 1–43. <https://doi.org/10.3301/GFT.2011.01>

- 720 Rossi, M., Reichenbach, P., 2016. LAND-SE: a software for statistically based landslide susceptibility zonation, version 1.0.
721 Geosci. Model Dev. 9, 3533–3543. <https://doi.org/10.5194/gmd-9-3533-2016>
- 722 Sarro, R., Mateos, R. M., Reichenbach, P., Aguilera, H., Riquelme, A., Hernández-Gutiérrez, L. E., Martín, A., Barra, A.,
723 Solari, L., Monserrat, O., Alvioli, M., Fernández-Merodo, J. A., López-Vinielles, J., Herrera, G. (2021). Geotechnics
724 for rockfall assessment in the volcanic island of Gran Canaria (Canary Islands, Spain). *Journal of Maps* 16(2), 605-613
725 (2020).
- 726 Santangelo, M., Gioia, D., Cardinali, M., Guzzetti, F., & Schiattarella, M. (2013). Interplay between mass movement and
727 fluvial network organization: An example from southern Apennines. *Italy Geomorphology*, 188, 54–67.
- 728 Schiattarella, M., Beneduce, P., Di Leo P., Giano, S.I., Giannandrea, P., Principe, C. (2005) - Assetto strutturale ed evoluzione
729 morfotettonica quaternaria del vulcano del Monte Vulture (Appennino lucano). *Boll. Soc. Geol. It.*, 124: 543-562.
- 730 Schlögel, R., Marchesini, I., Alvioli, M., Reichenbach, P., Rossi, M., Malet, J.-P., 2018. Optimizing landslide susceptibility
731 zonation: Effects of DEM spatial resolution and slope unit delineation on logistic regression models. *Geomorphology*
732 301, 10–20. <https://doi.org/10.1016/j.geomorph.2017.10.018>
- 733 Servizio Geologico d'Italia (1970a) - Carta Geologica d'Italia alla scala 1:100.000 – F. 34 Breno. E.I.R.A., Firenze
- 734 Servizio Geologico d'Italia (1970b) - Carta Geologica d'Italia alla scala 1:100.000 – F. 186 S. Angelo dei Lombardi. Ercolano
735 (Napoli)
- 736 Servizio Geologico d'Italia (1968a) - Carta Geologica d'Italia alla scala 1:100.000 – F. 36 Schio. Bergamo.
- 737 Servizio Geologico d'Italia (1965) - Carta Geologica d'Italia alla scala 1:100.000 – F. 185 Salerno. E.I.R.A., Firenze
- 738 Servizio Geologico d'Italia (1969) - Carta Geologica d'Italia alla scala 1:100.000 – F. 199 Potenza. Roma.
- 739 Servizio Geologico d'Italia (1964) - Carta Geologica d'Italia alla scala 1:100.000 – F. 163 Lucera. E.I.R.A., Firenze.
- 740 Servizio Geologico d'Italia (1955) - Carta Geologica d'Italia alla scala 1:100.000 – F. 265 Mazzara del Vallo. Firenze.
- 741 Servizio Geologico d'Italia (1970c) - Carta Geologica d'Italia alla scala 1:100.000 – F. 220 Verbicaro. Ercolano (Napoli)
- 742 Servizio Geologico d'Italia (1968b) - Carta Geologica d'Italia alla scala 1:100.000. F. 122 Perugia. Bergamo.
- 743 Servizio Geologico d'Italia (1970d) - Carta Geologica d'Italia alla scala 1:100.000 - F. 198 Eboli. Roma.
- 744 Servizio Geologico d'Italia (1970e) - Carta Geologica d'Italia alla scala 1:100.000 – F. 187 Melfi. Ercolano (Napoli).
- 745 Servizio Geologico d'Italia (2004) - Carta geologica d'Italia interattiva. Interactive geological map of Italy: 1:100.000. 3 CD.
746 M. AMANTI, R. BONTEMPO, P. CARA (a cura di). 1a edizione, Realizzato da Etruria innovazione.
- 747 Servizio Geologico d'Italia (1972) - Carta Geologica d'Italia alla scala 1:50.000, F. 027 Bolzano, Firenze.
- 748 Servizio Geologico d'Italia (1977) - Carta Geologica d'Italia alla scala 1:50.000, F. 028 La Marmolada, Firenze.
- 749 Servizio Geologico d'Italia (2002) - Carta Geologica d'Italia in scala 1:50.00, F. 132-152-153, Bardonecchia.
- 750 Servizio Geologico d'Italia (2005a) - Carta Geologica d'Italia alla scala 1:50.000, F. 503 Vallo della Lucania. APAT, Roma.
- 751 Servizio Geologico d'Italia (2005b) - Carta geologica d'Italia alla scala 1:50.000, F. 256 Rimini. APAT, Roma.

- 752 Servizio Geologico d'Italia (2005c) - Carta Geologica d'Italia alla scala 1:1.250.000. APAT, S.EL.CA., Firenze.
- 753 Servizio Geologico d'Italia (2005d) - Carta Geologica d'Italia alla scala 1:50.000, F. 215 Bedonia. APAT, Roma.
- 754 Servizio Geologico d'Italia (2006) - Carta Geologica d'Italia alla scala 1:50.000, F. 214 Bargagli. APAT, Roma.
- 755 Servizio Geologico d'Italia (2008) - Carta Geologica d'Italia alla scala 1:50.000, F. 058 Monte Adamello. APAT, Roma.
- 756 Servizio Geologico d'Italia (2009) - Carta Geologica d'Italia alla scala 1:50.000, F. 031 Ampezzo. ISPRA, Roma.
- 757 Servizio Geologico d'Italia (2009) - Carta Geologica d'Italia alla scala 1:50.000, F. 599 Patti. ISPRA, Roma.
- 758 Servizio Geologico d'Italia (2010) - Carta Geologica d'Italia alla scala 1:50.000, F. 258-271 San Remo. ISPRA, Roma.
- 759 Servizio Geologico d'Italia (2010) - Carta Geologica d'Italia alla scala 1: 50.000, F. 504 Sala Consilina. ISPRA, Roma.
- 760 Servizio Geologico d'Italia (2010) - Carta Geologica d'Italia alla scala 1:50.000, F. 228 Cairo Montenotte. ISPRA, Roma.
- 761 Servizio Geologico d'Italia (2011) - Carta Geologica d'Italia alla scala 1:50.000, F. 99 Iseo. ISPRA, Roma.
- 762 Servizio Geologico d'Italia (2011) - Carta Geologica d'Italia alla scala 1:50.000, F. 089 Courmayeur. ISPRA, Roma.
- 763 Servizio Geologico d'Italia (2011) - Carta Geologica d'Italia alla scala 1:50.000, F. 587-600 Milazzo-Barcellona P. di G.,
- 764 S.EL.CA., Firenze.
- 765 Servizio Geologico d'Italia (2011) - Carta Geologica d'Italia alla scala 1:1.000.000. ISPRA, Roma.
- 766 Servizio Geologico d'Italia (2012) - Carta Geologica d'Italia alla scala 1:50.000, F. 564 Carbonia. ISPRA, Roma.
- 767 Servizio Geologico d'Italia (2012) - Carta Geologica d'Italia alla scala 1:50.000, F. 098 Bergamo. ISPRA, Roma.
- 768 Servizio Geologico d'Italia (2012) - Carta Geologica d'Italia alla scala 1: 50.000, F. 489 Marsico Nuovo. ISPRA, Roma.
- 769 Servizio Geologico d'Italia (2014) - Carta Geologica d'Italia alla scala 1: 50.000, F. 505 Moliterno. ISPRA, Roma.
- 770 Servizio Geologico d'Italia (2015) - Carta Geologica d'Italia alla scala 1:50.000, F. 555 Iglesias. ISPRA, Roma.
- 771 Servizio Geologico d'Italia (2015) - Carta Geologica d'Italia alla scala 1: 50.000, F. 580 Soverato. ISPRA, Roma.
- 772 Servizio Geologico d'Italia (2015) - Carta Geologica d'Italia alla scala 1:50.000, F. 070 Monte Cervino. ISPRA, Roma.
- 773 Servizio Geologico d'Italia (2016) - Carta Geologica d'Italia alla scala 1:50.000, F. 280 Fossombrone. ISPRA,
- 774 Roma.
- 775 Tavarnelli E. (1997). Structural evolution of a foreland fold-and-thrust belt: the Umbria-Marche Apennines, Italy. *Journal of*
- 776 *Structural Geology*, 19, 523-534
- 777 **Tavarnelli, E., Renda, P., Pasqui, V., Tramutoli, M. (2003a). The effects of post-orogenic extension on different scales:**
- 778 **an example from the Apennine–Maghrebide fold-and-thrust belt, SW Sicily. *Terra Nova*, 15, 1-7, 2003.**
- 779 **Tavarnelli, E., Renda, P., Pasqui, V., Tramutoli, M. (2003b). Composite structures resulting from negative inversion:**
- 780 **an example from the Isle of Favignana (Egadi Islands). *Bollettino della Società Geologica Italiana*, 122, 319-325.**
- 781 Trigila, A., Iadanza, C., & Spizzichino, D. (2010). Quality assessment of the Italian landslide inventory using GIS processing.
- 782 *Landslides*, 7(4), 455–470. <https://doi.org/10.1007/s10346-010-0213-0>

783 UNESCO-IUGS (2016) – International Stratigraphic chart (versione aggiornata reperibile nel sito:
784 <http://www.stratigraphy.org/index.php/ics-chart-timescale>)

785 Vanmaercke, M., Panagos, P., Vanwalleghem, T., Hayas, A., Foerster, S., Borrelli, P., Rossi, M., Torri, D., Casali, J., Borselli,
786 L., Vigiak, O., Maerker, M., Haregeweyn, N., De Geeter, S., Zgłobicki, W., Bielders, C., Cerdà, A., Conoscenti, C., de
787 Figueiredo, T., Evans, B., Golosov, V., Ionita, I., Karydas, C., Kertész, A., Krása, J., Le Bouteiller, C., Radoane, M.,
788 Ristić, R., Rousseva, S., Stankoviansky, M., Stolte, J., Stolz, C., Bartley, R., Wilkinson, S., Jarihani, B., Poesen, J.
789 (2021). Measuring, modelling and managing gully erosion at large scales: A state of the art. *Earth-Sci. Rev.* 103637.
790 <https://doi.org/10.1016/j.earscirev.2021.103637>

791 Vezzani, L., Festa, A., Ghisetti, F.C., 2010. Geology and tectonic evolution of the central-southern Apennines, Italy, Special
792 paper. Geological Society of America, Boulder, Colo.

793 Vignaroli, G., Mancini, M., Bucci, F., Cardinali, M., Cavinato, G. P., Moscatelli, M., Putignano, M. L., Sirianni, P., Santangelo,
794 M., Ardizzone, F., Cosentino, G., Di Salvo, C., Fiorucci, F., Gaudiosi, I., Giallini, S., Messina, P., Peronace, E.,
795 Polpetta, F., Reichenbach, P.,...Stigliano, F. (2019). Geology of the central part of the Amatrice Basin (Central
796 Apennines, Italy). *Journal of Maps*, 15(2), 193–202. <https://doi: 10.1080/17445647.2019.1570877>.

797 Vojtek, M., Vojteková, J. 2019.: Flood Susceptibility Mapping on a National Scale in Slovakia Using the Analytical Hierarchy
798 Process. *Water* 2019, 11, 364. <https://doi.org/10.3390/w11020364>

799
800
801
802
803
804
805
806
807
808
809
810
811
812
813
814
815
816

817 **APPENDIX**

818 **Data acquisition procedure**

819 ISPRA exhibits a REST service for the publication of spatial data (Table 1, ID 9). The acronym REST stands for
820 "REpresentational State Transfer", which is an architectural style to develop services using the http data transfer protocol. In
821 particular, ISPRA uses the ArcGIS REST API, the Advanced Programming Interface REST developed by ESRI through the
822 proprietary ArcGIS Online platform. The ESRI API can be queried through specific http requests (for example of GET type,
823 in which the service address is followed by a series of key-value information) that allow, for example, to obtain the
824 representation in JSON (JavaScript Object Notation) format of geometries (geospatial layer features) and associated attributes.
825 Normally this service is limited to the return of a maximum number of features for each request. The acquisition of the database
826 required (i) knowledge of the REST service APIs and (ii) a procedure for the automatic download of subsets of data, which
827 cannot be downloaded in a single piece by design of the website, and (iii) merging of all of the subsets into a single vector
828 map. To execute the download, we prepared a script to download subsets of 100 polygons (geometric features) for each single
829 call to the service, using the Linux *wget* command. The procedure is simple, and consists of a loop in which, at each iteration,
830 a number (Δ) of polygons (100, in the actual case), out of the 300,000 total available polygons. Given that the API of the REST
831 service database was unknown to us, we followed a trial-and error procedure to obtain a working script. Downloaded data
832 consisted of 2,927 files in GeoJSON format, which we converted to a single ESRI Shapefile using the GDAL/OGR library.
833